1958

A study of the capacties of swirl-type nozzles

Gilbert Edward Gearhart
Lehigh University

A STUDY OF THE CAPACITIES OF SWIRL-TYPE NOZZLES

By

GILBERT EDWARD GEARHART

A STUDY OF THE CAPACITIES OF SWIRL-TYPE NOZZLES

by

Gilbert Edward Gearhart

A Report of Research

Presented to the Graduate Faculty of Lehigh
University in partial fulfillment of the
requirements for the degree Master of Science

Lehigh University
Bethlehem, Pennsylvania

1958

A REPORT

Submitted to the Chemical Engineering Faculty

of Lehigh University in partial fulfillment of the

requirements for the degree of Master of Science

Subject: A STUDY OF THE CAPACITIES OF SWIRL-TYPE NOZZLES

Submitted by: Gilbert Edward Gearhart

Department of Chemical Engineering

Accepted by   _Cwclump_   _8/8/58_
               Professor in Charge   (date)

            AlanSFaust
            Head of the Department   (date)

i

Acknowledgements

The author wishes to express his gratitude to Dr. Curtis W. Clump, faculty advisor, for his helpful leadership and advice during the course of this investigation. Thanks too are due William Szulborski and Paul E. Tax for their helping hands and suggestions when most needed.

Table of Contents

I Abstract

A preliminary investigation aimed at developing a useful correlation for predicting flow capacity from atomizing nozzles as a function of the physical properties of the fluid being sprayed and nozzle design has been initiated.

An SAE 90 gear oil, having wide viscosity variations with temperature, was atomized from a Type SL Spraying Systems Co. nozzle. Atomization pressure was varied from 150 to 1900 psia. The nozzle orifices employed were 0.042 and 0.055 inches in diameter. Over the range of temperature investigated the oil viscosity varied from 35 to 215 centipoises.

By correcting for temperature rise through the nozzle and nozzle specifications the collected data can be tentatively correlated by:

$$\left(\frac{Q}{\mu_L d_o}\right) \left(\frac{L}{d}\right)^{2/3} = 16.33 \left(\frac{\Delta P g_c d_o^2 \rho_L}{\mu_L^2}\right)^{0.48}$$

II INTRODUCTION

The process of fluid atomization is gaining popularity and importance in the chemical and automotive industries as well as other leading fields. Spray drying, spray cooling, spray extraction and absorption, and fuel injection are some examples of the variety of applications which the atomization process is being used for today.

The aim of the atomization process is to break up a liquid or a slurry jet into a multitude of small drops. Hence, the surface area of the liquid would be greatly increased in preparation for its subsequent evaporation, combustion, or drying. Lord Rayleigh (9) in 1878 formulated the earliest acceptable principles involved in the break up of a liquid jet. Since that time much effort has been spent in investigating the drop-size distribution resulting from atomizing nozzles. Knowledge of this distribution permits the calculation of the surface area formed and hence opens the door to better nozzle design.

When choosing a particular nozzle for use in any industrial process, considerable time and money is usually spent in preliminary pilot plant testing. Data is collected concerning nozzle capacity for the liquid to be used over the desired operating range, and a study is made of the drop-size distributions involved. A search of the literature reveals that no one correlation exists which relates the capacity of standard nozzles as a function of nozzle dimensions and the physical properties of the wide range of liquids that are used

for atomization. It is apparent that such a correlation would have an excellent potential in today's expanding technology. Nozzle pre-testing would be lessened to a great degree if an accurate correlation of this type existed.

The development of a generalized correlation will involve extensive research with the different types of spray nozzles available and must include the entire range of liquids used for spraying. This investigation was begun in an attempt to initiate a research program aimed at getting information for useful correlations.

III LITERATURE REVIEW

A. Theoretical:

The important theoretical considerations involved in any study of atomization are varied and complex. The direction and outcome that a hypothesis will take depends, among other things, upon the type of atomization technique. Four main techniques that are available are as follows:

1. Atomization by means of a centrifugal or swirl-type pressure nozzle.

2. Impingement atomization, where two liquid jets impinge, or a single jet impinges on a solid surface.

3. Spinning-disk atomization, where a liquid is discharged at a high velocity from the periphery of a rapidly rotating disk.

4. Pneumatic atomization, where a jet is disintegrated by a high velocity gas stream.

This report deals with atomization through a swirl-type pressure nozzle. The main contributing force acting to cause atomization is the spinning motion imparted to the liquid prior to its issuance from the nozzle. Hence the empirical relationships governing atomization from a swirl-type nozzle will differ from the other types of nozzles listed above even though the variables affecting atomization such as orifice opening, pressure, viscosity of the liquid, etc. may be the same.

The principles behind atomization, the characteristics of swirl-type nozzles, and the variables affecting atomization will be mentioned briefly along with an approach to the

correlations that this investigation hopes to develop.

1. **Principles of jet breakup:**

    The study of the causes of atomization is best understood by first considering the breakup of a simple jet. Lord Rayleigh (9) in 1878 predicted the conditions necessary to cause the collapse of a low velocity jet. Neglecting friction of the surrounding medium and viscous forces of the liquid, he deduced that a small symmetrical disturbance about the axis of an irrotational jet would cause breakup when the amplitude of the disturbance grew to one-half of the diameter of the undisturbed jet. See Figure (1-a). Mathematically this may be written as

$$\alpha = \alpha_{0} e^{qt} \tag{1}$$

where:
α = amplitude of the disturbance at time t
α_{0} = initial amplitude of the disturbance
q = time rate of growth of the amplitude of disturbance

The maximum value of q, and hence the maximum value of α, according to Rayleigh is

$$q_{max.} = 0.345 \sqrt{\frac{\sigma_{L}}{\rho_{L} R_{0}^{3}}} \tag{2}$$

where:
R = initial jet radius
σ_{L} = liquid surface tension
ρ_{L} = liquid density

Furthermore, Rayleigh calculated the average drop size at breakup and found it to be equal to $1.89 d_{0}$, or nearly twice the diameter of the undisturbed jet. See Figure (1-b). This confirmed his deduction.

FIGURE 1

circumference of undisturbed jet
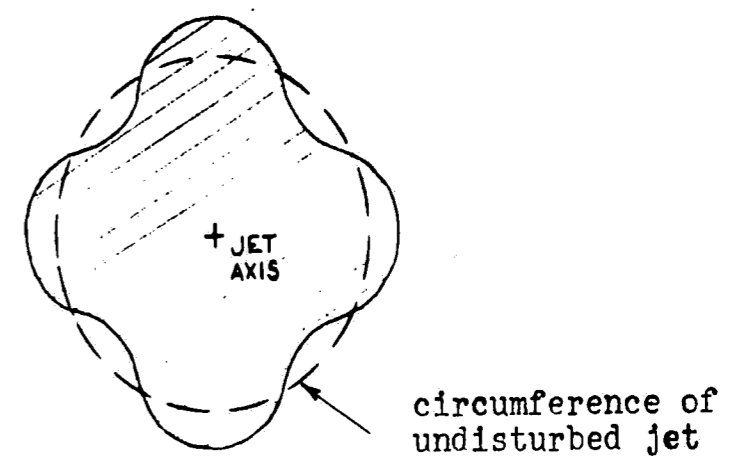
a. Idealized representation of initial symmetrical, circumferential disturbance around a liquid jet.
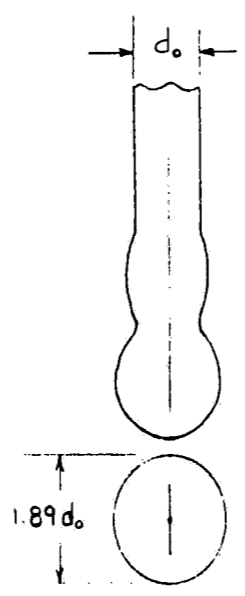
b. Idealized jet breakup
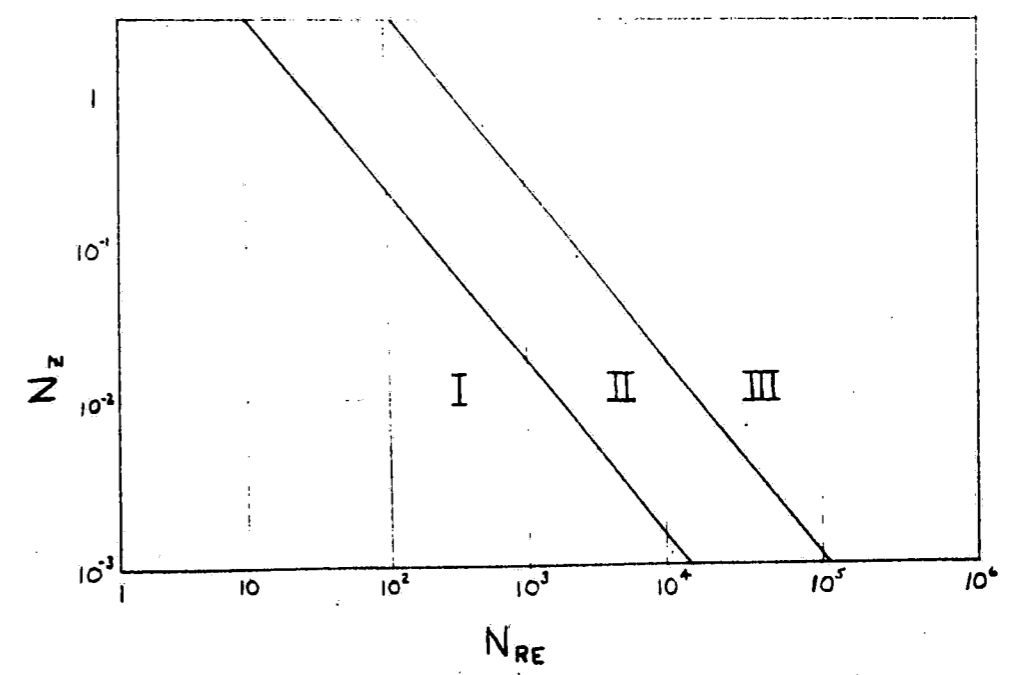
c. Jet breakup as a function of Reynolds number and liquid properties.

Rayleigh's simplified picture of jet stability has been substantiated by several investigators. However, his work only provides a starting point, since the conditions existing in an actual jet are not so simple. For example the flow is almost always turbulent, viscous forces are present, and the effect of surrounding air is not negligible.

Haenlein (4) in 1931 investigated the effect of air friction on a jet as the discharge velocity was increased with the aid of high speed photography. He found that air friction promoted increased oscillations about the jet axis which favored a shorter breakup distance of the jet. As the jet velocity was increased, breakup occurred as a result of wave formation on the surface of the jet. These waves were caused by increased air friction. When the velocity reached a value typical of that found in actual practice, complete and immediate disintegration of the jet took place immediately after the liquid left the orifice. Haenlein offered no explaination of this last observation.

Ohnesorge (7) extended Rayleigh's work by including the effect of viscous forces while still neglecting the influence of the surrounding air. He considered that jet breakup was dependent upon jet diameter, jet velocity, liquid density, surface tension, and viscosity. With the aid of dimensional analysis he predicted the breakup mechanism of a jet as a function of the Reynolds number $vd_o \rho / \mu_l$ and the so-called Z number, $\mu_l / \sqrt{\sigma_l \rho \, d_o}$. By plotting these groups, three distinct zones were found, Figure (1-c). Zone I follows Rayleigh's

mechanism closely, where the viscous forces can be considered negligible. In zone II the jet takes on a twisted appearance. And finally, zone III occurs abruptly when atomization takes place.

Summarizing the work of these and other investigators, the following conclusions apply to the mechanism of jet breakup:

1. If a liquid jet is turbulent throughout, it will breakup without any outside force. Disintegration will occur as soon as surface tension is overcome.

2. A semiturbulent jet will collapse after it leaves the nozzle only when the turbulent part forges ahead of the laminar part.

3. A laminar jet needs an external force as predicted by Rayleigh.

4. Disintegration is favored by air friction.

5. As the liquid viscosity increases, the jet breakup distance increases.

6. As the pressure increases the breakup distance decreases.

2. Characteristics of swirl-type nozzles:

Swirl-type pressure nozzles are characterized by a hollow conical spray pattern. As previously mentioned, the atomizing action is caused largely by the spinning motion imparted to the liquid within the nozzle and does not depend upon the relative motion between the surrounding air and the liquid. The spinning motion can be accomplished by a variety of ways.

Consider a conical chamber within the nozzle with a grooved-core insert. Refer to Figure (2-a). As the liquid enters the chamber through the grooved core, a radial, tangential, and an axial velocity component result.

The conditions existing in the spin chamber constitute what is known as a free vortex; i.e., the fluid flows in a horizontal circular path with no torque applied. Examining the tangential velocity distribution in a free vortex, the expression for the point tangential velocity component v_t is given by

$$v_t \approx 1 / r \qquad\qquad (3)$$

where:
r = radius of curvature of a differential element of fluid.

Equation (3) requires an infinite velocity at $r = 0$, or at the center of the chamber. Since this is not possible, the spinning liquid cavitates and an air core is created at the chamber axis which extends through the orifice. Refer to Figure (2-b).

As the liquid leaves the nozzle it ceases to spin, and the radial momentum causes the liquid to move radially outward while it is also moving in an axial direction. This gives rise to the conical spray pattern, which is a function of the resulting axial and tangential velocity components. Thus the swirling action and the resulting cone angle are of fundamental importance in causing atomization.

The following stages in the atomization of a liquid are characterized by swirl-type nozzles with increasing pressure:

FIGURE 2

grooved core insert

grooved inlet to
spin chamber

spin chamber

d_o
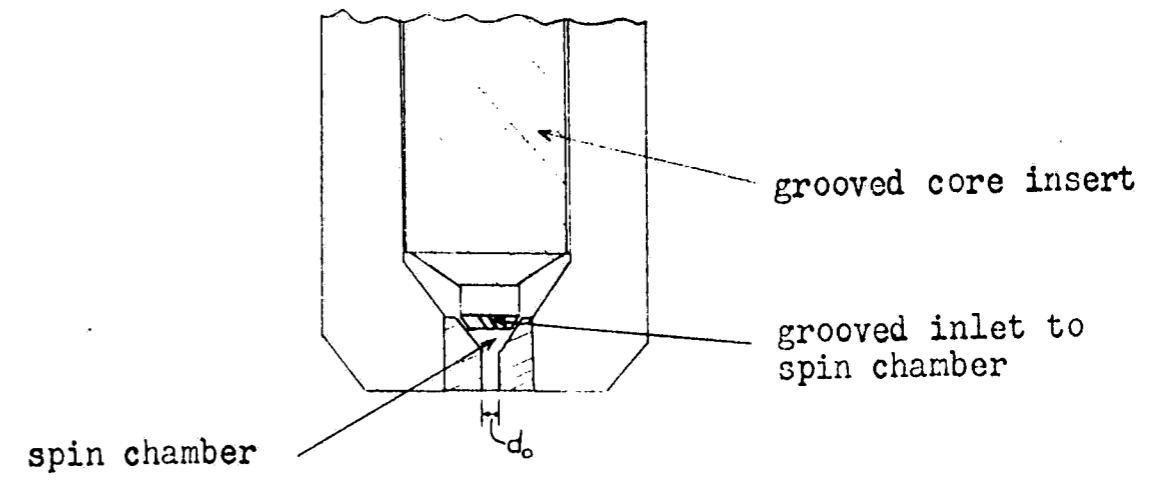
a. Pressure nozzle with a grooved-core insert to impart spin.

R_o

R_d
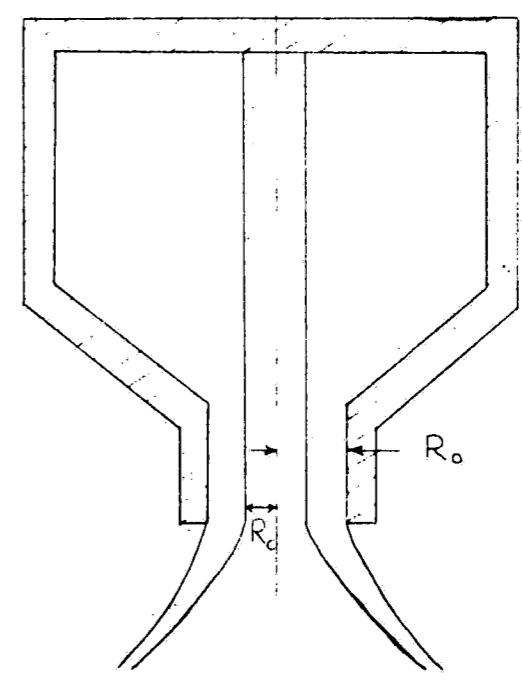
b. Diagram suggesting the air core in a swirl-type pressure
nozzle.

1. The liquid issues from the orifice in a corkscrew fashion with insufficient swirl velocity to produce an air core.

2. A helical pattern is seen, with breakup due to ligament formation resulting from unstable films.

3. The air core forms; as the liquid attempts to open into a spray the surface tension draws it back, and a tulip formation results.

4. The tulip opens into the characteristic hollow-cone spray.

3. <u>Variables affecting spray performance</u>:

Having considered the basic underlying principles in the atomization process and the effects of nozzle construction, it is desirable to investigate the importance of the physical variables that affect atomization, with particular emphasis upon spray performance. The prime concern here is the effect of these variables upon the flow capacity through the nozzle.

The physical variables that are considered are:

1. Injection pressure, P

2. Velocity through the nozzle, v_o, based on the orifice diameter, d_o

3. Liquid properties

   a. density, ρ

   b. surface tension, σ

   c. viscosity, μ_L

4. Dimensions of the nozzle

a. orifice diameter, d_o

b. air core diameter, d_c

These variables are closely related, and the final outcome of
nozzle capacity is affected to some degree by each one. Spray-
ing is a dynamic situation, and even though the above variables
are interrelated some of them may be considered insignificant
compared to others. It is therefore desirable to determine
the relative importance of each variable.

For the case of a liquid being atomized, a plot of
the log of the pressure versus the log of the flow rate results
in a straight line. This criterion was kept in mind when
taking the nozzle capacity data for this report and was used
as a check upon data reliability.

The operating pressure plus the orifice opening will
certainly place a limit on nozzle capacity in any given situ-
ation. Within the nozzle considerable kinetic energy, $v_o^2/2g_c$,
is imparted to the liquid to form the unstable configuration
which eventually breaks up into a spray. Therefore v_o, based
upon the diameter of the orifice, as well as being an indication
of the degree of atomization is also a correlation of the
weight rate of flow, Q. However, it is incorrect to base the
velocity on d_o directly. The presence of an air core must not
be overlooked. The actual value of the velocity for a constant
pressure situation depends upon the size of the air core. The
air core has been found to be independent of pressure and
dependent upon the physical properties of the liquid, namely
viscosity (5).

The coefficient of discharge for a nozzle is repre-

sented by the flow number, F_n, where

$$F_n = Q / \sqrt{P} \tag{4}$$

This equation does not account for viscosity. Giffin and Muraszew (3) have shown that the coefficient of discharge for viscous liquids deviates from the theoretical value of Equation (4). Viscosity is a measure of fluid resistance to shear. As the viscosity increases, fluid friction increases within the nozzle. As friction increases, the coefficient of discharge increases. This phenomenon is not immediately apparent. However, the presence of friction results in a decrease in the tangential and axial velocities. The decrease in the tangential velocity means less swirling; hence the diameter of the air core decreases and there is more area for flow through the nozzle. This effect in air core reduction more than compensates for the reduced axial velocity at lower injection pressures. As long as atomization occurs, the capacity of the nozzle increases up to the point where a forced vortex occurs and an air core can no longer form. At high pressures the reduction in axial velocity plays a great part and the coefficient of discharge will begin to decrease for a viscous liquid. Thus, liquid viscosity is a key variable and it will predominate prior to jet breakup.

The density and surface tension of most liquids used for spraying show a rather slight change with temperature. Further, their effects on nozzle capacity are considered insignificant, even for wide temperature changes (3). The effect of these variables is recognized in the disintegration process

after the liquid has left the nozzle. A liquid of high density
will produce a more compact and penatrating spray, which may
be difficult to atomize and disperse in the surrounding medium
(3). Surface tension forces oppose any distortion in the
surface of a liquid, and hence retard ligament formation and
jet disintegration (3). Liquid surface tension has its greatest
effect in the study of particle size and will not be considered
in this investigation.

4. Correlations:

The variables and their effects upon nozzle capacity
can be related empirically with the use of dimensionless
groups. This use of dimensional analysis has several advantages.
It allows the bringing together in a neat grouping all the
important variables. Once the dimensionless groups have been
established, it should be possible to predict the change in
flow rate of a liquid through the nozzle with the aid of the
groupings.

The variables that will be considered significant in
this investigation are: (a) nozzle diameter (b) velocity
through the nozzle (c) liquid viscosity (d) liquid density
and (e) injection pressure.

Several different dimensionless groups may be
established from either all or some of the five variables.
See the calculations section for a development of these groups.
It must be pointed out that even though each grouping will
differ in form from the others, that no one can be considered

more theoretically correct than any other. However, to determine which grouping sucessfully presents any collected data in the most logical manner, it is necessary to plot each grouping versus nozzle capacity. The best presentation will then be the smoothest plot.

The weight-flow distribution, which is sometimes referred to as patternation, may be determined simply by collecting and measuring the sprayed liquid at various positions beneath the nozzle. A plot of weight/unit time of liquid collected versus distance from the nozzle axis provides a simple qualitative picture of the spray pattern. In general, the spray pattern has not been found to be sharply defined due to turbulence created by the surrounding air as the liquid filament breaks up. The mean spray angle, however, may be determined. Using the axial velocity component v_o, and the mean angle the tangential velocity component v_t can be calculated. The availability of such weight-flow data, then, is important when designing a spray tower. Also, the knowledge of spray distribution is a necessary step in establishing the proper weighting factors for any study of particle size distribution.

B. <u>Summary of previous work</u>:

Consiglio and Sliepcevich (1) have correlated the mass flow rate for water using a commercial pressure type atomizer as a function of the injection pressure, viscosity, density, and orifice diameter. Their results take the following

form:

$$\frac{d_o^2 \Delta P_\ell}{\mu_L^2} = k''' \left(\frac{\rho_L Q}{d_o \mu_L} \right)^a \tag{5}$$

Similar work has been done by other investigators in this field (5)(10). However, the following limitation exists. The correlations relating flow rate to the variables affecting spraying exist only for water and a very limited amount of other liquids. No generalized correlation is available that is independent of the liquid being sprayed. The advantages of such a generalized correlation are quite evident:

1. Existing gaps in the knowledge about spraying would be nicely filled in.

2. Much time and expense involved in the preliminary stages of pilot plant work would be eliminated.

3. It should be possible to improve nozzle design, which would lead to more efficient nozzles.

Several methods for determining the patternation have been used. Perhaps the most common method was employed by Dumas and Laster (2), where a series of 40 tubes were placed equidistant in a semicircle under Spraying Systems' Whirljet nozzle. It has been maintained that this procedure introduced errors because of the targeting effect (5), causing some liquid to flow around the collectors and not be measured. As a solution, an attempt was made to measure the impact force

of the spray on a rotating cantilever arm. This method does not appear to be sucessful, since additional errors result from measuring the momentum of any entrained air, which also impinges on the arm.

The spray chamber used in this investigation was designed to minimize collection errors in the hope of obtaining the most accurate picture of the spray pattern.

IV SCOPE OF INVESTIGATION

It is the concern of this investigation to develop a simplified correlation between nozzle capacity, a parameter of the nozzle, and some function of the physical properties of SAE 90 gear oil. Socony Mobil Company supplied the oil, which was chosen because of its large change in viscosity over a relatively narrow temperature range. The physical properties of this oil were experimentally determined and are found in Appendix A. Similarly all equipment specifications may be found in Appendix B.

It is hoped that this investigation will lay the ground work for further research encompassing the wide variety of liquids that are used in the atomization process. Another goal of this investigation is to ascertain the effect that the physical properties of the oil have on the spray pattern.

No research has been made in the measurement of drop-size distribution. This study is a problem in itself and shall be considered outside the range of this investigation.

V APPARATUS & EXPERIMENTAL TECHNIQUE:

A. Apparatus

Refer to Figure (3) for a schematic diagram of the apparatus and to Figure (4) for the design of the spray chamber and collection system. The apparatus was designed and constructed with simplicity in mind and precision and reproducibility of the data the goal.

The oil reservoir (A) consisted of a thirty gallon drum open at the top. Available steam at 5 psig supplied heat to the oil through 8 turns (turn diameter = 15") of 1/2" O.D., type K, copper tubing. The heating coils (B) were readily converted to cooling coils by disconnecting the steam line and attaching a cold water line. A Lightning Mixer (C) was used to insure uniform temperature in the reservoir. The oil temperature in the reservoir was controlled by an American springloaded steam valve (D) in line with the steam coils. The valve was actuated by a vapor pressure thermal bulb that was immersed in the reservoir and attached to the valve by flexible cabling.

A Pesco Hydraulic Gear pump (E) supplied a constant volume of oil. The pump was driven by a General Electric 5 HP motor (F) using a direct chain and sprocket arrangement. Because of the speed at which the motor turned over, a constant oil drip was needed on the chain to keep it from overheating. On the low pressure side of the pump a Cuno Auto-Klean filter (G) was installed. This filter effectively removed grit and

FIGURE 3

DIAGRAM OF APPARATUS
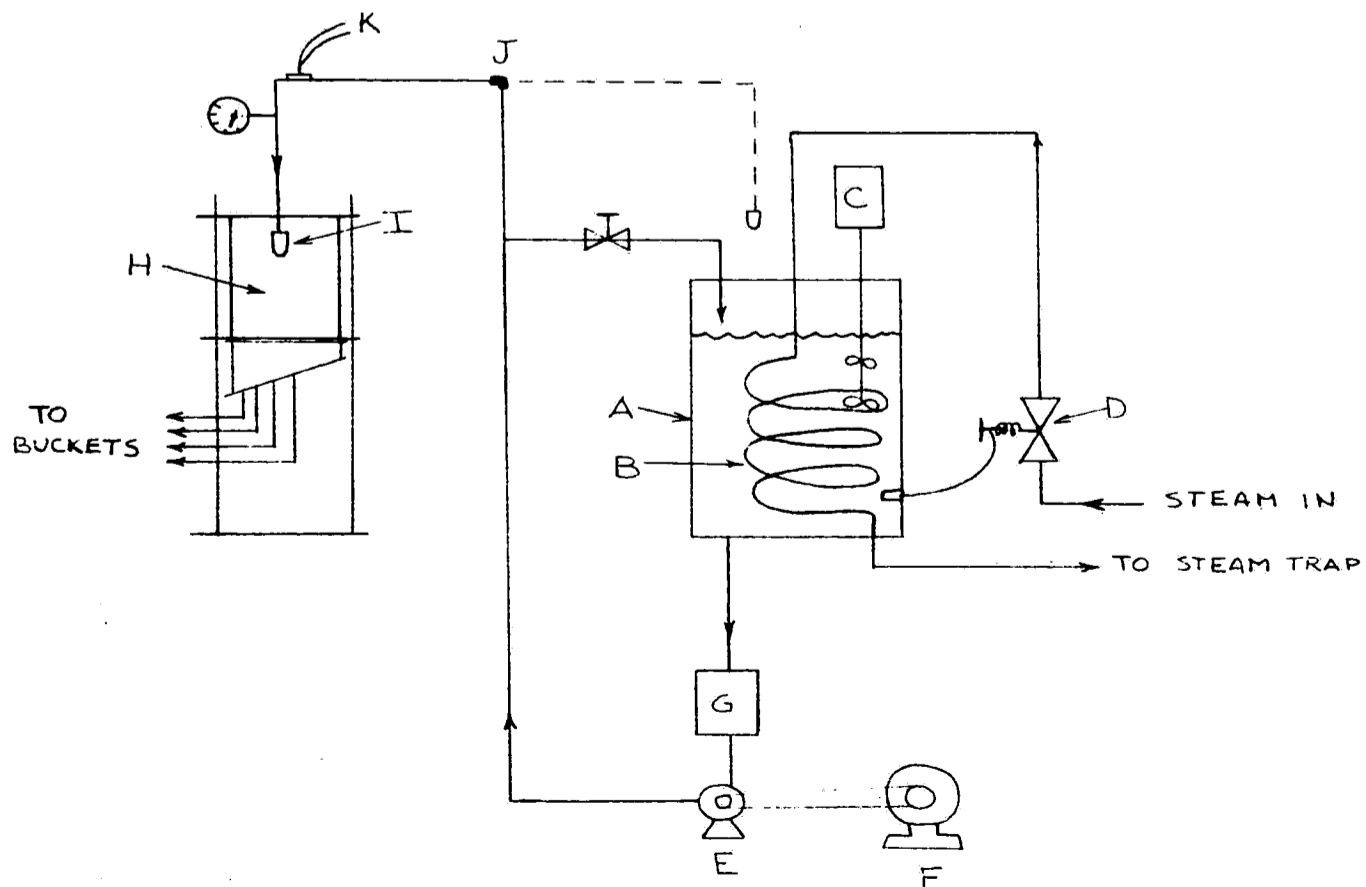
CODE:

A. OIL RESERVOIR

B. STEAM COILS

C. AGITATOR

D. STEAM CONTROL VALVE

E. PUMP

F. MOTOR

G. FILTER

H. SRAY CHAMBER

I. NOZZLE

J. SWIVEL JOINT

K. THERMOCOUPLE

FIGURE 4
Spray chamber and collection device

6.0"
5.2"
4.24"
3.0"

OIL

TO BUCKETS

1. Separation plate (divided into four equal areas)
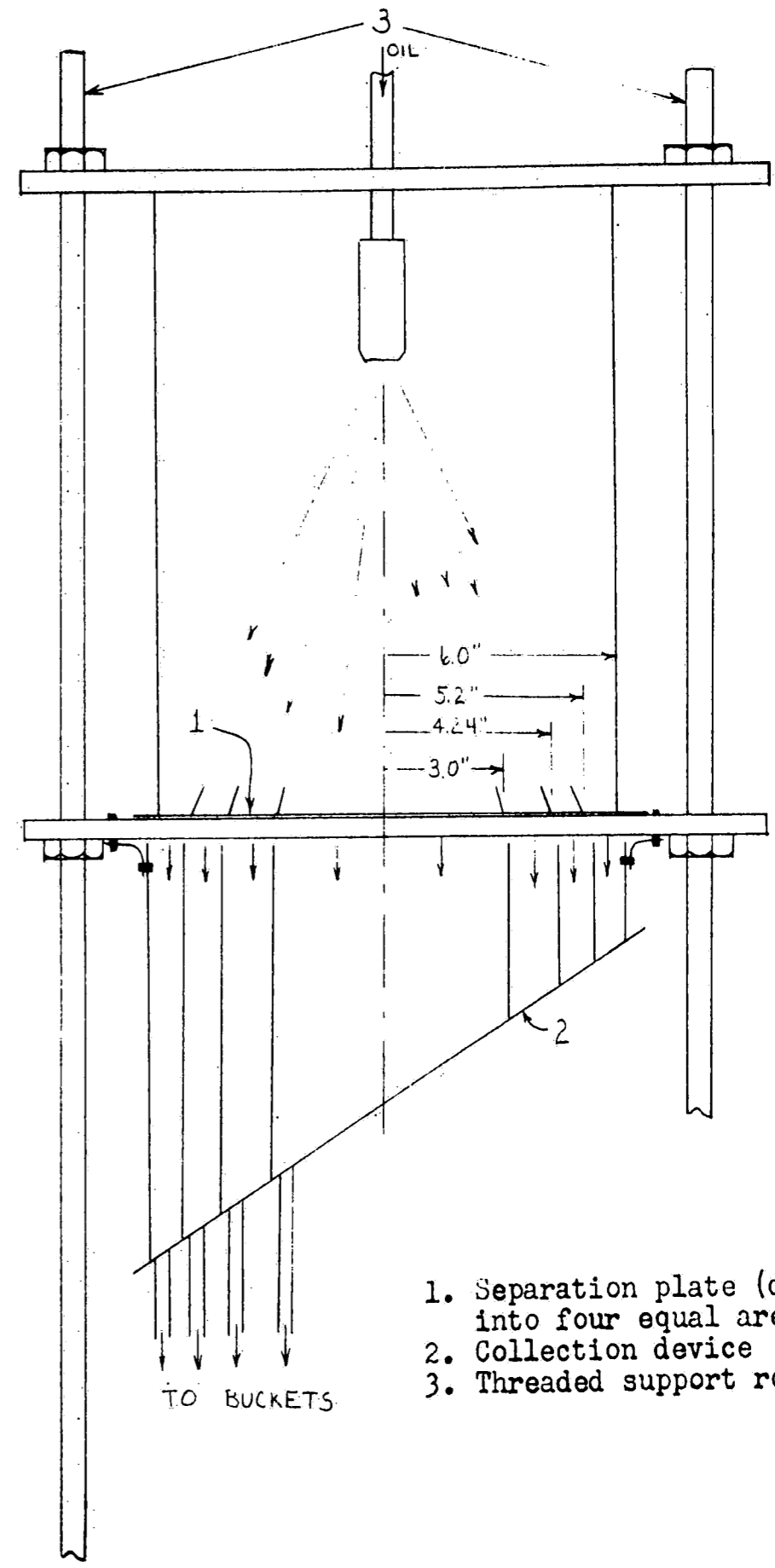2. Collection device
3. Threaded support rods

lint particles larger than 0.005 inches.

A Spraying System atomizing nozzle (I) was used to atomize the oil. Refer to Figure (5) for a diagram of nozzle construction. The nozzle is a swirl type with removable orifice and core. By inserting different combinations of orifices and cores, a wide range of flow rates was obtained with the same nozzle body.

The pressure of the oil feeding to the nozzle was regulated by means of a needle valve installed in the by-pass line. There exists a relatively large resistance to flow in the nozzle as compared to that resistance in the by-pass line. Consequently with the needle valve open wide, nearly all the oil returned to the reservoir tank, and the pressure before the nozzle was essentially atmospheric. As the needle valve was slowly closed, more oil was forced through the nozzle and the pressure increased correspondingly. A maximum pressure of 2000 psig upstream from the nozzle was obtained in this manner. Immediately upstream from the nozzle an iron-constantan thermocouple was installed to record the oil temperature.

The spray chamber was designed to collect the sprayed oil from equal annular areas at the base of the chamber. From this arrangement, a quantitative picture of the distribution pattern at a right angle to the hollow cone spray can be obtained. The wall of the spray chamber was a 15" length of acyrlic lucite tubing, 12" inside diameter, with a 1/4" wall thickness. The base plate of the chamber was constructed from 1/32" copper sheeting and was divided into four equal annular areas of 28.3 sq. in. each. The areas were separated from

FIGURE 5

Spraying Systems' spray drying nozzle, Type SL
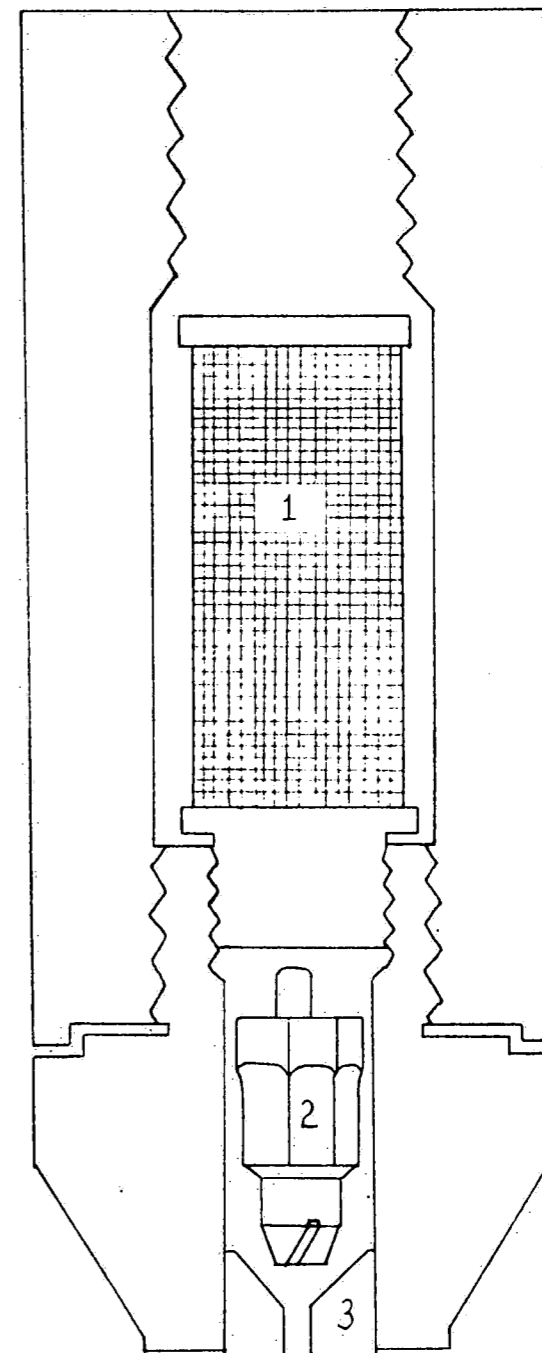
1. Strainer (oil flows from outside to inside)
2. Replaceable core
3. Orifice insert

each other by means of struts 1" high, which were inclined so as to be in direct alignment with an average spray angle of 65°. The oil fell directly through the base plate into a collection device which captured the oil from each area. The oil from each of the areas then fell by gravity through tygon tubing into three-gallon galvanized iron buckets for weighing.

The lucite tubing and the base plate were placed between two steel plates 15" square, 1/4" thick, with a 12" circle cut out of the center of each plate. The collection device was bolted in place beneath the bottom steel plate. The entire arrangement was supported by bolting the steel plates between four 1/2" threaded steel rods. The nozzle was centered in the chamber, but fixed in height owing to the piping. However, by raising or lowering the chamber on the threaded support rods, it was possible to vary the distance between the nozzle and the base plate if need be.

All of the piping on the high pressure side of the pump was schedule 80 steel pipe. A high pressure swivel joint upstream from the nozzle permitted the nozzle to be transferred out of the chamber to the reservoir if desired. However, this advantage was not taken during the course of data runs.

B. Experimental Procedure

The experimental procedure found to be most successful in obtaining reproducible data was as follows: The mixer was turned on. Next, the steam was turned on, with the spring on the steam valve preset at the proper tension to produce the

desired temperature, and the oil in the reservoir was allowed to come up to temperature. The oil drip on the chain was started and the motor was turned on with the needle valve in the by-pass line open wide. The needle valve was slowly closed, bringing the system to the desired pressure for the particular run. The system was allowed to come to equilibrium, i.e. when the temperature upstream from the nozzle became steady. Usually this temperature was no more than 2 to 4 Fahrenheit degrees below the reservoir temperature. The other criterion for equilibrium was the steady-state flow of oil from each of the four collection areas.

While waiting for equilibrium, the oil from all the areas was collected in one bucket. As this bucket became full, an auxilliary bucket was used. It was possible to pour the oil from the full bucket into the reservoir without affecting the upstream nozzle temperature to any great degree.

It was learned that for pressure above 500 psig the pump performed a sufficient amount of work on the oil to raise the oil temperature fairly high. At these conditions, the oil returning to the reservoir was hot enough to raise the reservoir temperature as much as a Centigrade degree a minute at the lower temperature runs, even with the steam turned off. Consequently, the steam coils were converted to cooling coils to insure a steady pre-nozzle temperature whenever needed.

Equilibrium was generally attained within ten minutes. A run was begun by simultaneously starting a stop watch and transferring the tygon tubing from each of the four areas into separate buckets. A maximum of a four second delay

occured between the starting of the watch and the transfer of the last tygon tube. During the course of a run, the pressure was held constant by regulating the needle valve. The reproducibility of data runs in terms of pressure versus flow rate was directly dependent upon how well pressure fluctuations were kept at a minimum. It was important, then, to keep a constant eye on the pressure gage. Temperature measurements were taken at intervals during the run. If any change in pre-nozzle temperature was noted, an average reading was used for the run.

The runs were ended by stopping the watch and at the same time returning the tygon tubes, in the same order as originally transferred, back to the single bucket. The needle valve was opened wide and the system was shut down. The buckets containing the oil from the four areas were weighed to the nearest ounce. It was then possible to determine the flow rate in lbs/hr at the particular pressure and temperature of the run. The runs were made sufficiently long enough to render insignificant any errors due to the weighing of the buckets or the transferring of the tygon tubes.

C. Calculations

As a means for planning the experimental program the significant variables concerned with the atomization mechanism have been grouped by dimensional analysis. For example:

$$Q = f (d_o, v_o, P, \rho_L, \mu_L) \tag{6}$$

where:
f = any function

One development is to neglect the compressibility of the liquid through consideration of the pressure. If the change in compressibility is considered insignificant, the pressure may be omitted from equation (6) with the result

$$Q = k\, d_o^a\, v_o^b\, \rho^c\, \mu_L^d \tag{7}$$

where:
Q = flow rate, lbs./sec.
k = a constant
a,b,c,d = exponents

The final form of the dimensionless groupings obtained from equation (7) by considering the exponent d to be independent is

$$\frac{d_o^2\, v_o\, \rho}{Q} = k'\left(\frac{d_o\, v_o\, \rho}{\mu_L}\right)^d \tag{8}$$

where:
k' = a constant

By plotting $d_o^2\, v_o\, \rho/Q$ versus $d_o\, v_o\, \rho/\mu_L$ on log log coordinates a straight line should result, the slope of which equals the exponent d. The constant k' is the value of $d_o^2\, v_o\, \rho/Q$ when $d_o\, v_o\, \rho/\mu_L$ is equal to one on the log coordinate.

The velocity v_o is considered dependent upon the injection pressure P. Hence by substituting the pressure for the velocity another result is

$$Q = z\, d_o^e\, \Delta P g_c^f\, \rho^g\, \mu_L^h \tag{9}$$

where:
z = a constant
$\Delta P g_c$ = pounds mass-ft./sec.^{2}-ft.^{2}
e,f,g,h = exponents

Then:

$$\frac{Q}{\mu_L d_o} = z'\left(\frac{\Delta P g_c\, d_o^2\, \rho}{\mu_L^2}\right)^e \tag{10}$$

where:
z' = a constant

The exponent e and the constant z' are found in the same manner described for d and k' by plotting equation (10).

Still another development would be to include all of the variables of equation (6):

$$Q = x \, d_o^i \, v_o^j \, \Delta P g_c^m \, \rho^n \, \mu_L^s \tag{11}$$

where:
x = a constant
i,j,m,n,s = exponents

Hence if m and s are taken to be independent

$$\frac{d_o^2 \, v_o \rho}{Q} = x' \left(\frac{\rho v_o^2}{\Delta P g_c} \right)^m \left(\frac{d_o \, v_o \rho}{\mu_L} \right)^s \tag{12}$$

where:
x' = a constant

The exponent m equals the slope of $\rho v_o^2 / \Delta P g_c$ versus $d_o^2 \, v_o \rho / Q$. to find s and x' plot $(d_o^2 \, v_o \rho / Q)(\rho v_o^2 / \Delta P g_c)^m$ versus $d_o \, v_o \rho / \mu_L$.

Equations (8), (10), and (12) are in reality modified drag coefficient equations. Equations (8) and (12), upon examination, are found to be meaningless. In both cases the left side of the equation $d_o^2 \, v_o \rho / Q$ is equal to one, since $d_o^2 \, v_o \rho = Q$. Therefore these two equations are not useful and will not be considered.

The usual practice in representing any fluid flow data is to plot a Reynolds number versus a drag coefficient $\Delta P g_c / \rho v^2$. Equation (10) is essentially this type of correlation, and it would appear to be a logical method of presenting the data of this and similar investigations. It will be of further interest to ascertain if the data of this investigation conforms to other forms of fluid flow data by plotting

$d_o \, \mathbf{v}_o \rho / \mu_l$ versus $\Delta P g_c / \rho_l \, \mathbf{v}_o^2$.

The temperature of the oil going through the nozzle will increase due to frictional forces dissipating heat to the oil. This temperature increase will cause a viscosity change. to determine the temperature rise through the nozzle, a standard energy balance is made around the nozzle:

$$H_1 + \frac{\mathbf{v}_1^2}{2g_c} + Z_1 + Q' - W' = H_2 + \frac{\mathbf{v}_2^2}{2g_c} + Z_2 \qquad (13)$$

The following assumptions are made:

1. The system is adiabatic, hence $Q' = 0$.

2. The change in elevation equals zero, or $Z_2 - Z_1 = 0$.

Hence equation (13) reduces to

$$H_1 - H_2 = \frac{\mathbf{v}_2^2 - \mathbf{v}_1^2}{2g_c} \qquad (14)$$

since no shaft work appears in the system. The initial velocity $\mathbf{v}_1$ in the pipe before the nozzle is known; the velocity $\mathbf{v}_2$ equals the velocity through the orifice $\mathbf{v}_o$, if we neglect the effect of the air core. The initial enthalpy H_1 at T_1 is used as the base enthalpy and will be taken as zero. Therefore H_2 may be calculated directly from equation (14). If a basis of one second operation is used, the temperature rise of the oil through the nozzle is

$$T_2 - T_1 = \frac{H_2}{C_p \, Q} \qquad (15)$$

where:
$C_p = $ BTU/lb.-°F

$T_2, T_1 = $ degrees Fahrenheit

This ΔT could also be evaluated using the mechanical energy balance and solving for the friction through the nozzle.

The spray pattern is obtained by plotting the lbs. per second of liquid collected from four equal annular areas situated under the nozzle versus distance from the nozzle axis.

VI Discussion of Results

In Table (8), Appendix C are the tabulated results
of four sets of data. Each set consisted of a series of runs
reported as pressure versus mass flow rate taken at constant
temperature for a particular orifice opening. Conditions for
sets I and II were: (a) Temperatures of 134 and 90°F
respectively, (b) Constant orifice diameter of 0.0035 ft.
For sets III and IV: (a) Temperatures of 90 and 132.5°F
respectively, (b) Constant orifice diameter of 0.00458 ft.
Thus, the experimental program was designed to investigate
the independent effect of each of the three variables pressure,
viscosity, and orifice opening upon the mass flow rate.

A. Effect of viscosity:

Consider, momentarily, the results plotted as the
drag coefficient $\Delta Pg_c/\rho\, v_o^2$ versus the Reynolds number on
logarithmic coordinates; refer to the solid lines in Figure 6.
As was mentioned, a plot of this type is the usual method for
presenting any fluid flow data. However, the results of this
investigation do not seem to follow any meaningful trend on
this type of plot. Sets II and IV are an indication of turbulent
flow, since these lines are at constant values of $\Delta Pg_c/\rho\, v_o^2$.
Set I which had the same orifice opening as II is inconsistant
with set II in that as the Reynolds number increases we move
from turbulent to non-turbulent conditions.

Keeping Figure 6 in mind, consider now the results
plotted as $Q/\mu d_o$ versus $\Delta Pg_c d_o^2 \rho /\mu^2$. Refer to the solid

FIGURE 6

DRAG COEFFICIENT — REYNOLDS NUMBER

SET	d_o	°F
I	0.0035 ft.	134
II	0.0035 ft.	92
III	0.00458 ft.	90
IV	0.00458 ft.	132.5
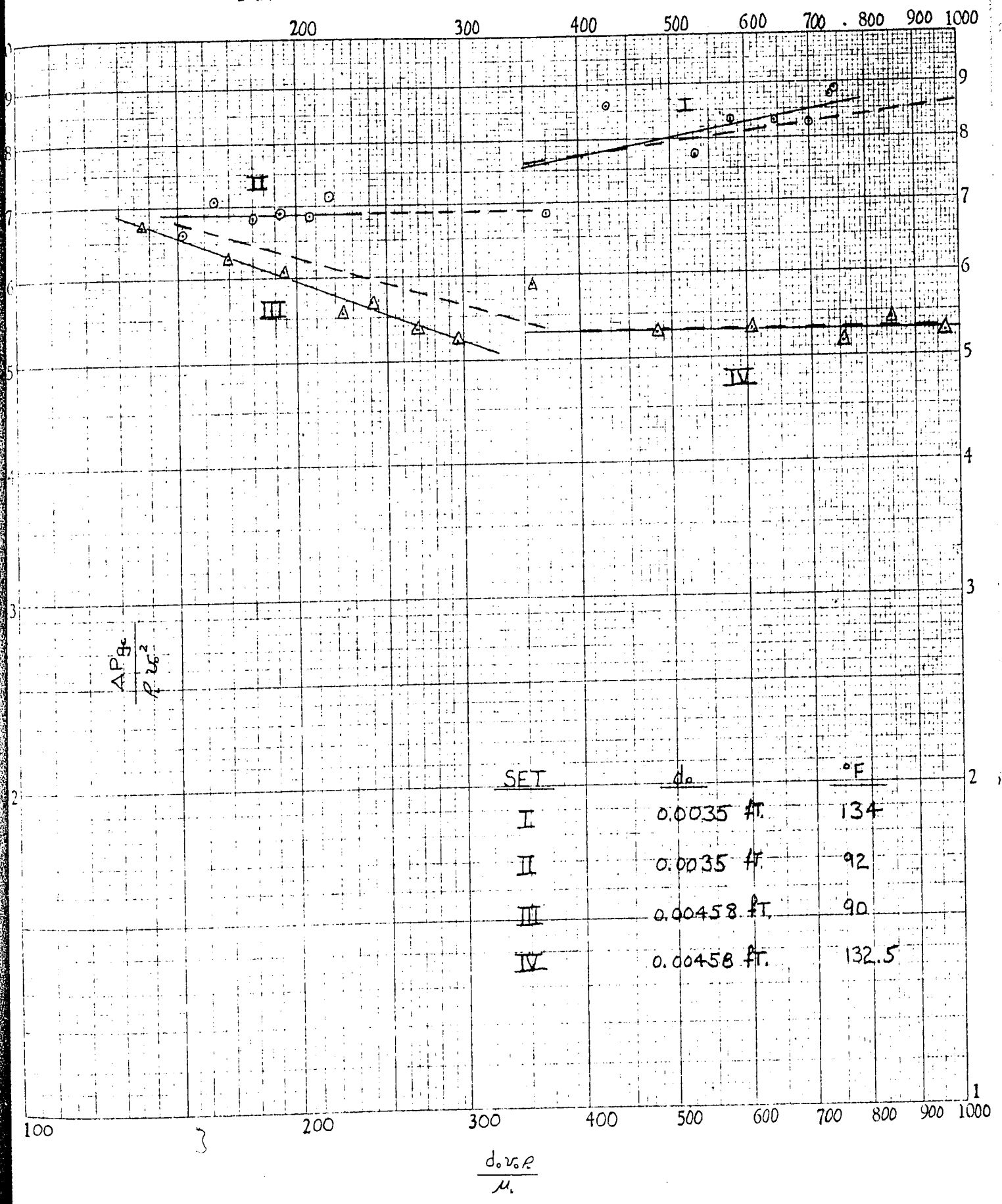
lines in Figure 7. The four sets appear to follow a definite trend. However, it is felt that sets I and II should be represented by a single line since the orifice opening 0.0035 ft. was used in both cases. Similar reasoning applies to sets III and IV, for which the orifice opening 0.00458 ft. was used. Therefore an attempt will be made to bring these respective sets together. The temperature readings used in this investigation were based on pre-nozzle conditions. It is therefore desirable to calculate the temperature rise through the nozzle from an energy balance, so that a more accurate value may be assigned to the viscosity of the oil issuing from the nozzle. The dotted lines in Figure 7 refer to the viscosity correction.

Consider sets I and II. As was suspected the viscosity correction brought these two sets very nicely together. In set II the temperature rise through the nozzle changed from $8.1^{\circ}F$ at a pressure of 900 psi to $11.6^{\circ}F$ at a pressure of 1900 psi. In set I the temperature rise was more marked and changed from $4.8^{\circ}F$ at 300 psi to $9.9^{\circ}F$ at 1700 psi. Refer to Appendix D for the calculations. Consequently the line representing set I was corrected more and sets I and II came into alignment. Sets III and IV upon correction conform very nearly to a single line. The only discrepancy appears at the lower pressure runs of set III.

Reconsider now the drag coefficient - Reynolds number correlation mentioned earlier. If a straight line is drawn through all the data of Figure 7 a slope of about 1/2 results. This would indicate that viscosity is cancelled from the

FIGURE 7

$$\frac{Q}{\mu_c d_0} \quad vs. \quad \frac{\Delta P g_c d_0^2 \rho}{\mu_c^2}$$

(DOTTED LINES REFER TO VISCOSITY CORRECTION)

$$\frac{\Delta P g_c d_0^2 \rho}{\mu_c^2}$$
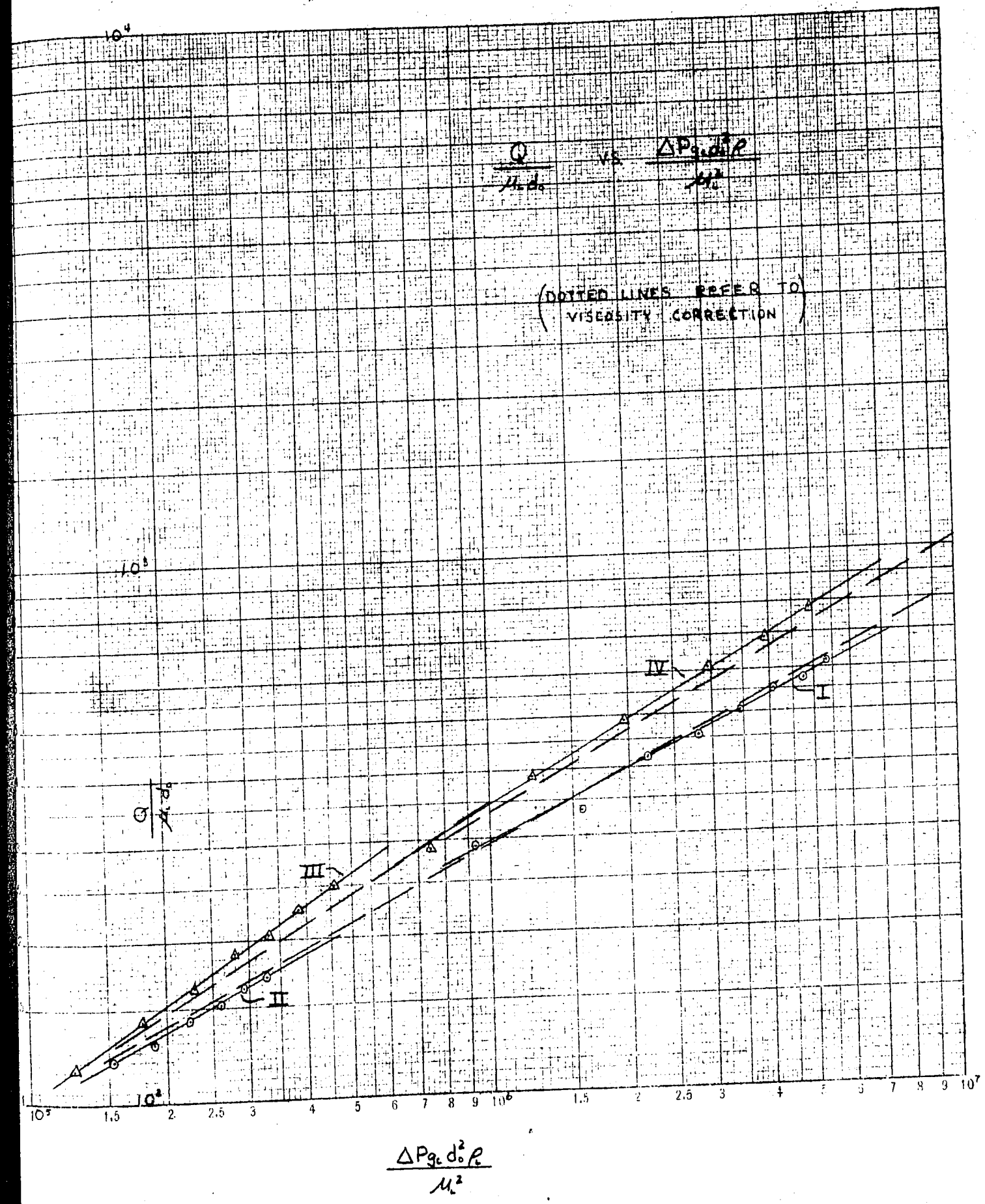
correlation of Figure 7 and full turbulence is indicated. It
is therefore doubtful at this time if the drag coefficient-
Reynolds number correlation of Figure 6 is of any use, since
according to this plot flow conditions appear to be not
completly turbulent as $\Delta Pg_c/\rho \ v_o^2$ is not constant. Even
with the viscosity change taken into account (the dotted lines),
this plot does not adequately represent the data of this
investigation. Hence, Figure 6 will not be considered any
further as a means of correlating the data of this investigation
at this time.

B. Effect of orifice diameter:

     The correction for temperature rise through the
nozzle has established a more accurate picture of flow conditions
as represented by Figure 7. However the corrected sets I and
II, and III and IV plot as two nearly parallel lines instead
of one. It should be possible to consolidate the four sets
into one by considering the effect of the independent variable
d_o. To do this an L/d ratio will be used, where L equals any
characteristic length of the orifice insert. For the time
being L is assumed constant for both the orifice inserts that
were used and is assigned the value one. This assumption will
be justified if the four sets of data in Figure 7 can be
brought together into a single line.

     Hence, the L/d correction will take the following
form:

$$\left(\frac{Q}{\mu_L d_0}\right) \left(\frac{L}{d}\right)^{e'} = x'' \left(\frac{\Delta P g_c d_0^2 \rho}{\mu_L^2}\right)^{f'} \tag{16}$$

To determine the value of the exponent e' a plot was made of the log L/d_0 for the two orifice diameters versus log $Q/\mu_L d_0$ at constant values of $\Delta P g_c d_0^2 \rho /\mu_L^2$. Refer to Figure 8 for this plot. The value of e' was chosen to be 2/3, as it more nearly brought the data of Figure 7 into a single straight line.

Figure 9 is the final result of the viscosity and the L/d corrections. The values of x'' and f' of equation (16) were calculated to be 16.33 and 0.48 respectively. In general, the data of this investigation have been grouped rather nicely into a single line as represented by Figure 9. Nevertheless the following limitations must be kept in mind:

1. The data of this investigation covers a narrow range and hence must not be relyed upon too heavily.

2. SAE 90 gear oil was the only liquid used. To further substantiate the validity of the correlation developed by this investigation the liquids of lower viscosity should be tested.

With respect to the second limitation, an attempt was made to include data reported by the Spraying Systems Co. in their Catalog No. 24 for water at 70°F, using the same nozzle and orifice diameters as were used in this investigation. However, the values calculated for $\Delta P g_c d_0^2 \rho /\mu_L^2$ were in the range 10^{10} while the values for $Q/\mu_L d_0$ were in the range 10^5. Spraying Systems reported only pressures of 1000 psi or greater. Water will atomize at pressures well below 1000 psi.

FIGURE 8

$$\frac{Q}{\mu_e d_o} \quad vs \quad \frac{L}{d}$$

SLOPE = -0.667

$$\frac{\Delta P_{g c} d_o^2 \rho_o}{\mu_e^2} = 2.0 \times 10^6$$

SLOPE = -0.75

$$\frac{\Delta P_{g c} d_o^2 \rho_o}{\mu_e^2} = 10^6$$

$$\frac{Q}{\mu_e d_o}$$

$$\frac{L}{d}$$

Figure 9

$$\left(\frac{Q}{\mu_i d_o}\right)\left(\frac{L}{d}\right)^{2/3} \quad vs \quad \frac{\Delta P g_o d_o^3 A}{\mu_i^2}$$
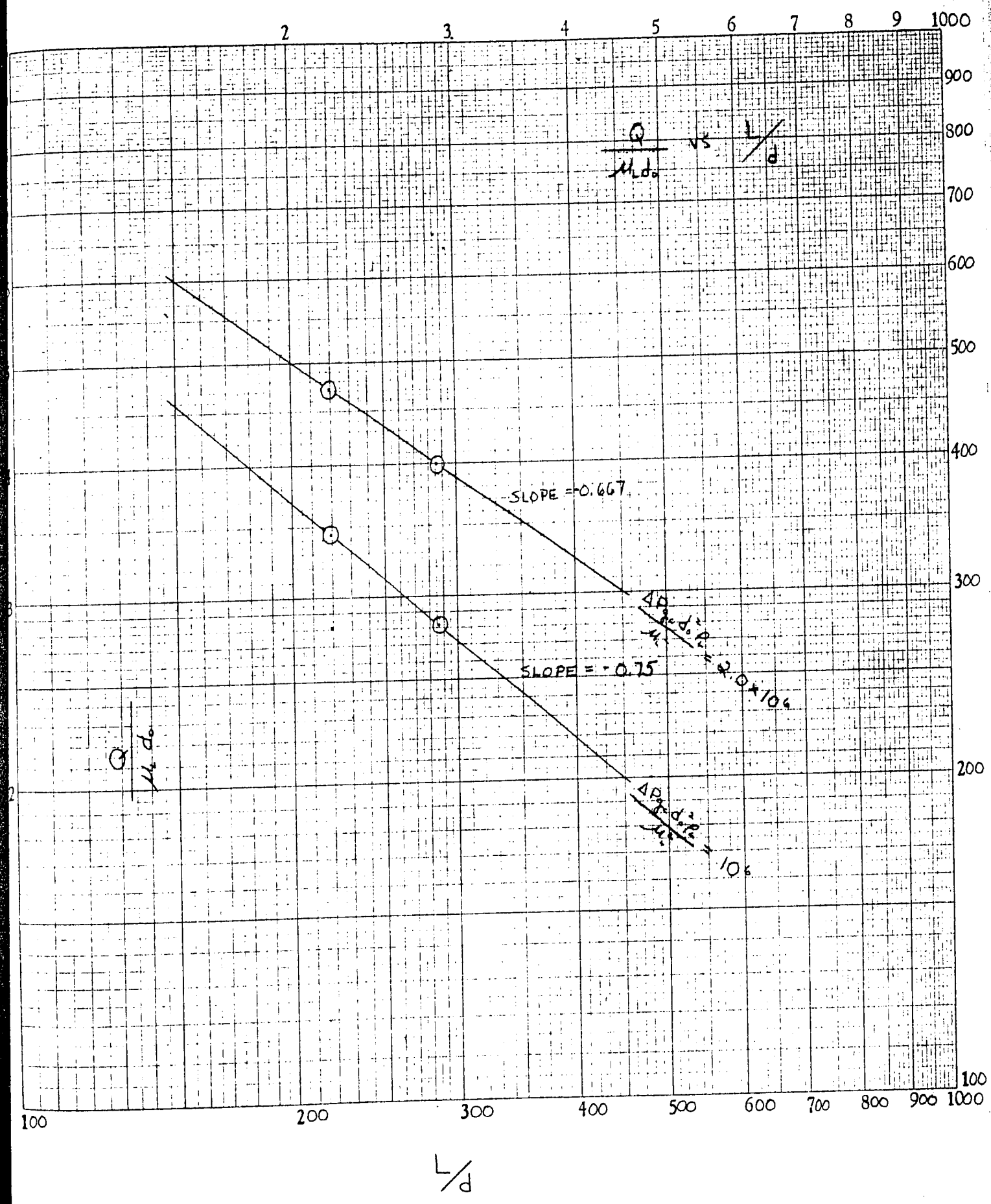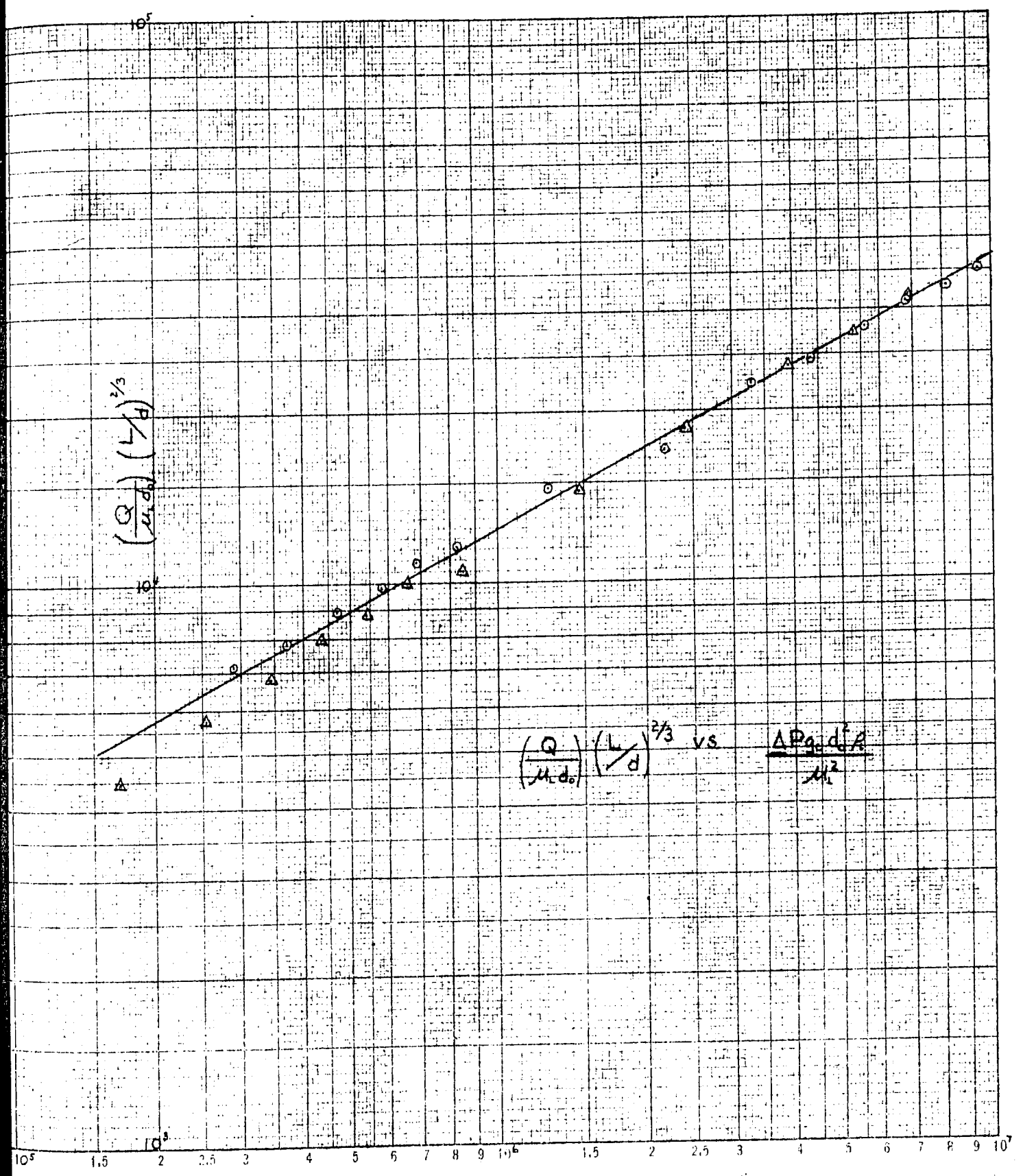
Therefore, since the data given by Spraying Systems is limited to higher pressures which give values that are well out of the range of Figure 9, it was decided not to extrapolate the data of this investigation to cover Spraying Systems' water data.

C. Spray pattern:

Figures 10, 11, 12, and 13 were chosen from the data of set III. Each figure represents the volume distribution of the spray taken at a right angle to the nozzle axis for the particular run chosen. As the pressure is increased it is clear that no logical pattern is developing. This can be explained from visual observations of each run. As the pressure was increased more turbulence within the chamber resulted from the effect of the surrounding air. The spray chamber as designed was too small. Hence much splashing occured, transfering a rather large portion of the liquid that would normally have been collected in the inner areas to the wall and roof of the chamber and hence to the outer collection area. As the pressure was increased, splashing increased.

It can be concluded that the spray chamber was designed ineffectively and that it was not possible to obtain an accurate picture of the spray distribution.

FIGURE 10

LBS/SEC. COLLECTED
VS.
INCHES FROM NOZZLE AXIS

(DATA RUN 53)

FIGURE 11

LBS./SEC. COLLECTED
VS.
INCHES FROM NOZZLE AXIS

(DATA RUN 56)

DISTANCE FROM NOZZLE AXIS, INCHES

FIGURE 12

LBS./SEC. COLLECTED

VS.

INCHES FROM NOZZLE AXIS

(DATA RUN 59)

DISTANCE FROM NOZZLE AXIS, INCHES

FIGURE 13

LBS./SEC. COLLECTED
VS.
INCHES FROM NOZZLE AXIS

(DATA RUN 61)

DISTANCE FROM NOZZLE AXIS, INCHES
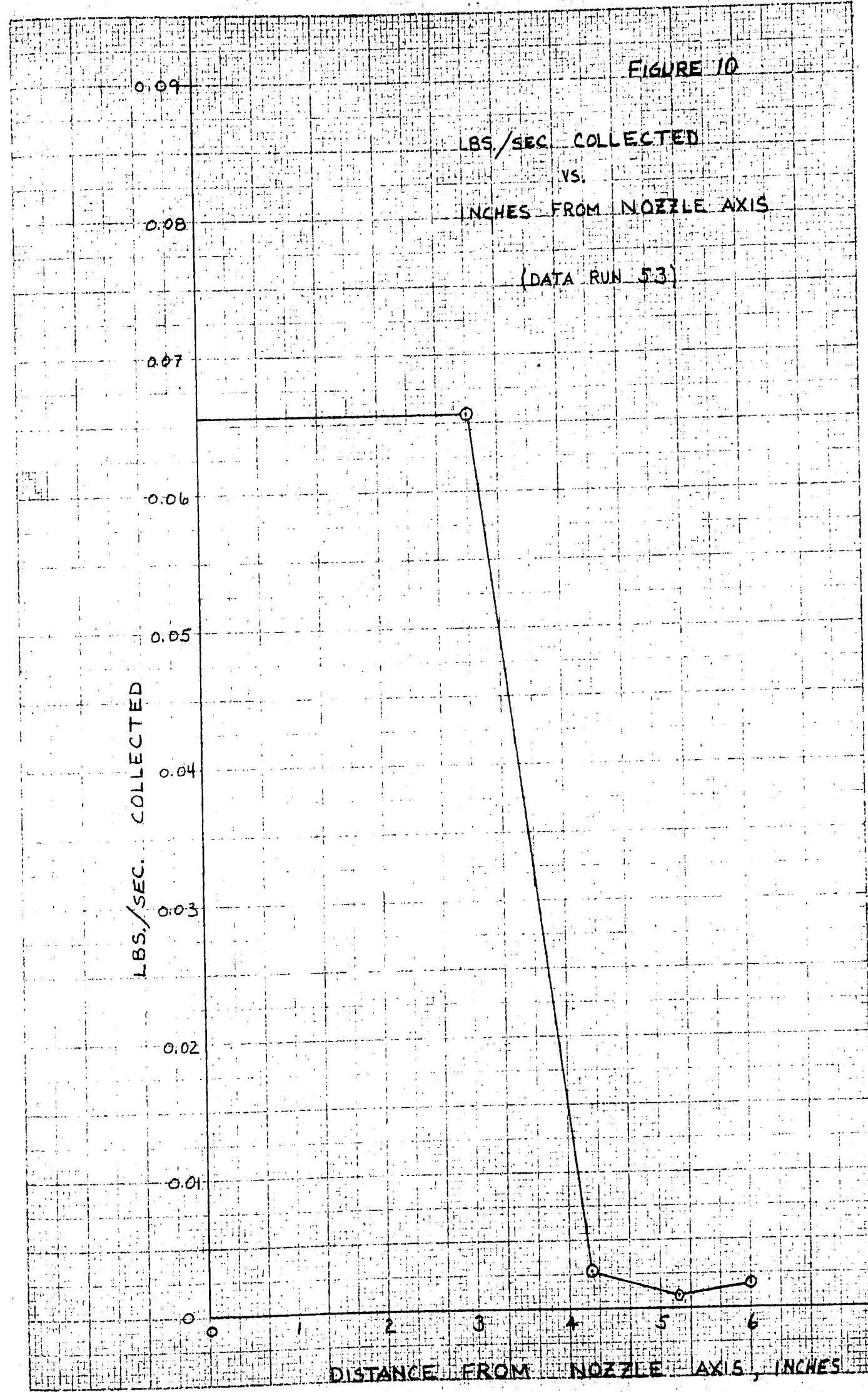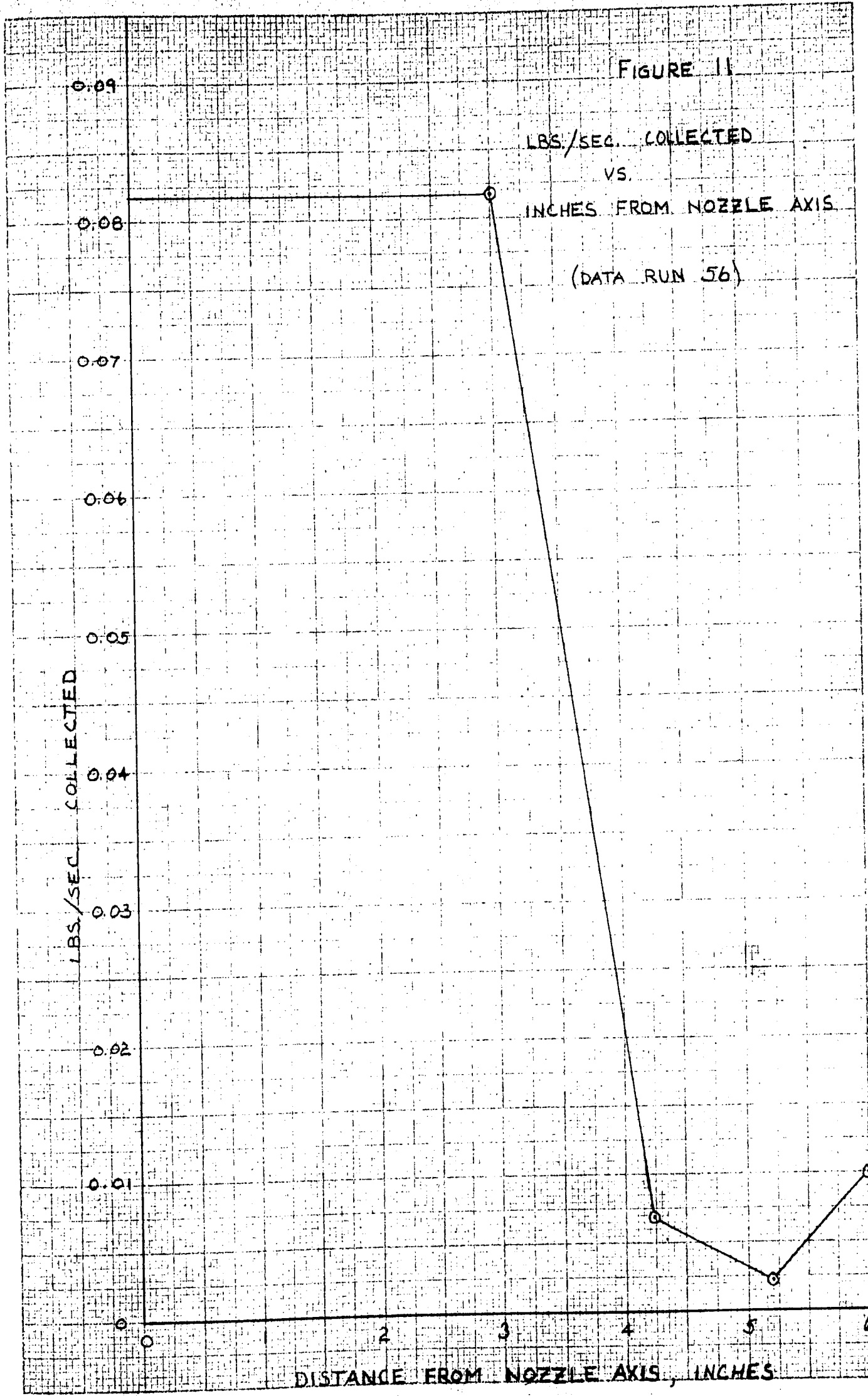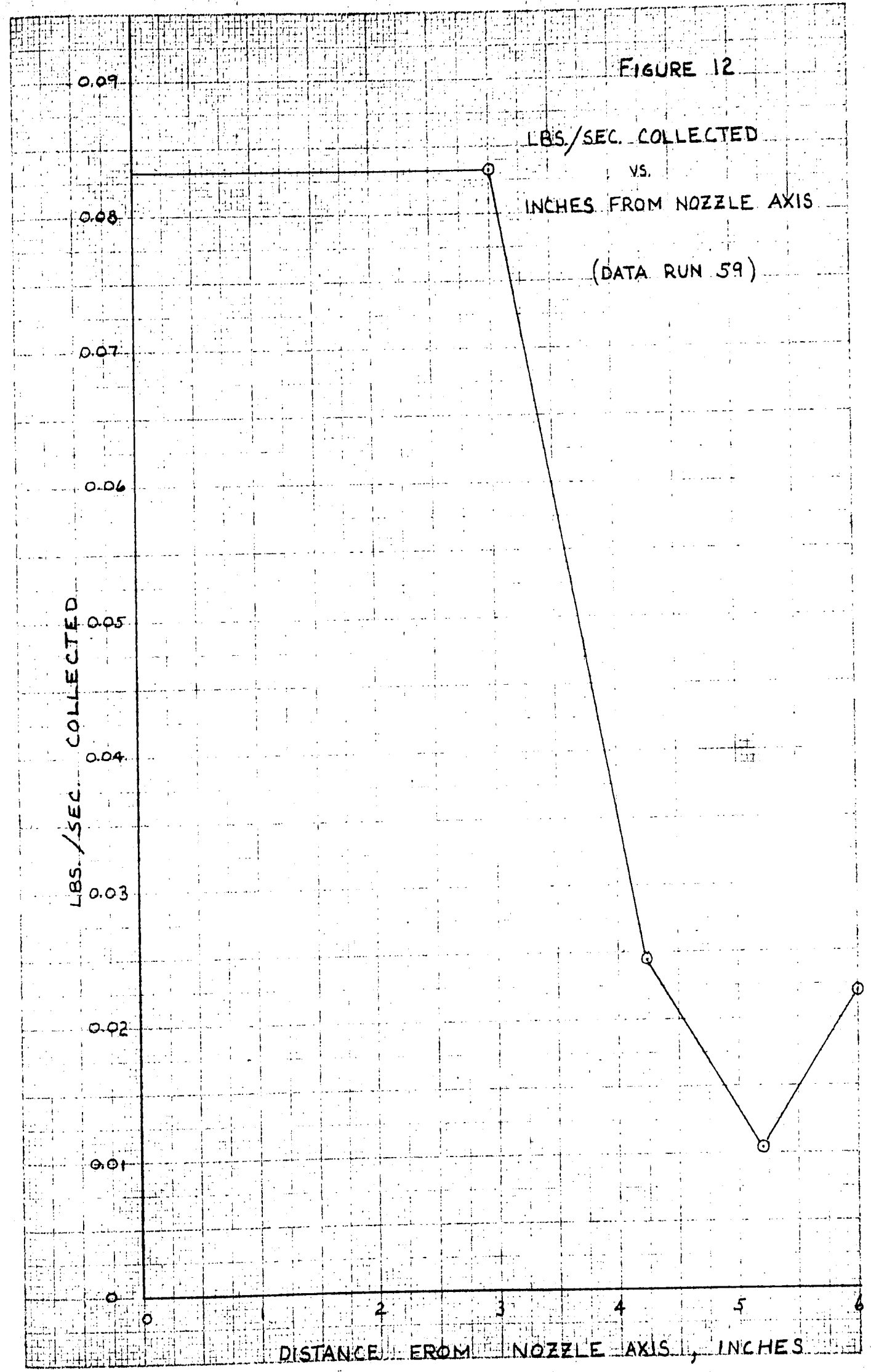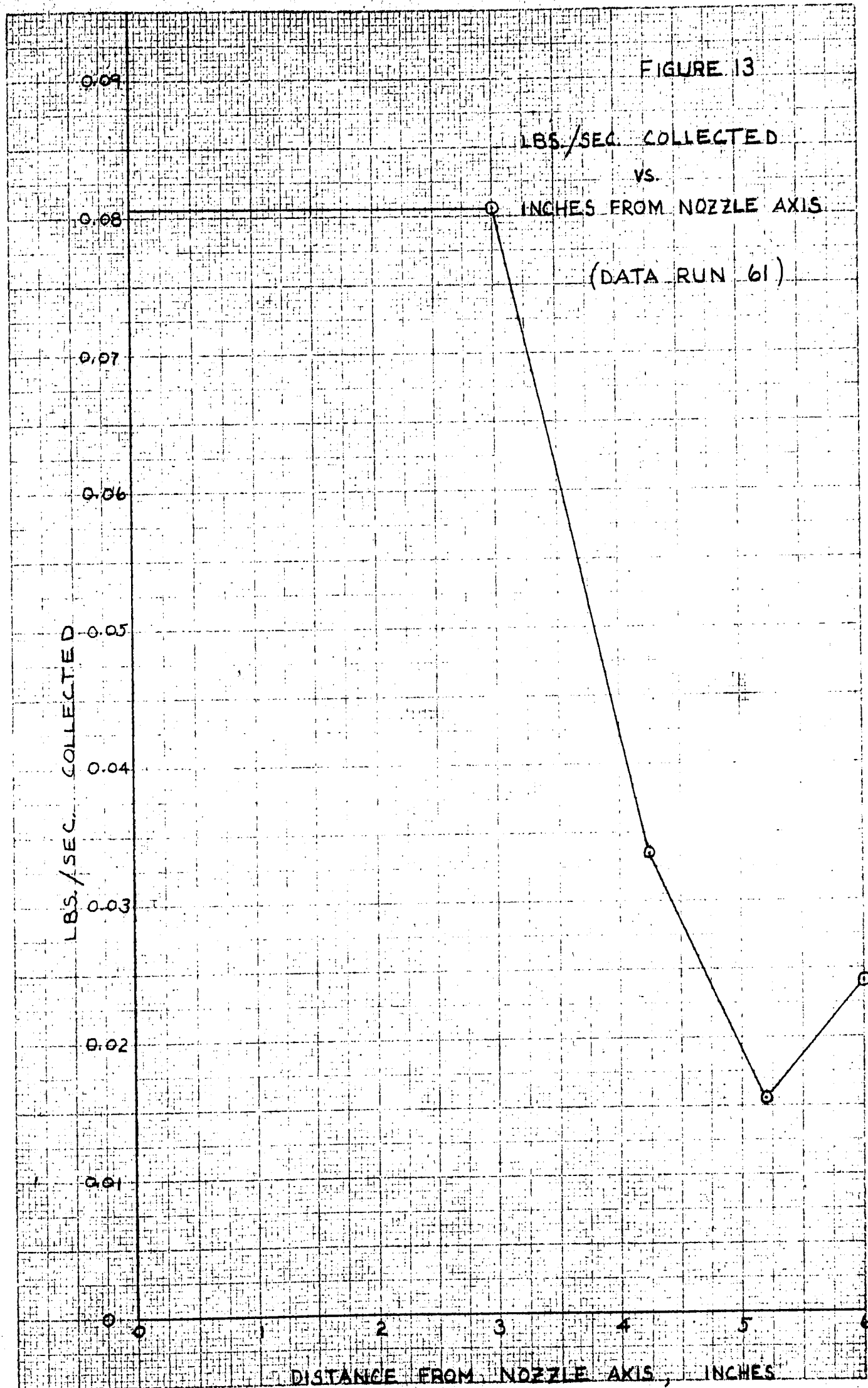
VII Conclusions and Recommendations

The results of this investigation show that the data correlates fairly well by the following equation:

$$\left(\frac{Q}{\mu_L d_O}\right)\left(\frac{L}{d}\right)^{2/3} = 16.33 \left(\frac{\Delta P g_c \, d_O^2 \, \rho_L}{\mu_L^2}\right)^{0.48} \tag{17}$$

Since this investigation is in reality a hydrodynamic flow study, it is not surprising that equation (17) takes the form of a modified drag coefficient - Reynolds equation. The fact that it does gives considerable weight to the validity of this investigation and the techniques used herein. However it must be stressed that the data of this investigation is limited and equation (17) represents a trend rather than an accurate correlation that could be applied to most fluids used in the atomization process.

The spray chamber as designed was too small to obtain an accurate picture of the spray pattern as a function of the injection pressure, the physical properties of the oil, and a dimension of the nozzle.

With the above results and limitations in mind, the following recommendations are made:

1. The spray chamber should be considerable larger. There is much turbulence caused by the high spray pressures and the effect of the surrounding air in the chamber. Hence to minimize collection on the walls and roof of the chamber it is recommended that a cubic chamber 6 ft. on a side be constructed.

The chamber should be constructed with windows
to allow continuous visual observations to be
made and a door for easy entry.

2. No detailed recommendations can be made at this
   time concerning the collection system to enable a
   spray pattern study of the improved chamber of
   recommendation 1. However it is felt that a
   slightly concave floor beneath the nozzle covered
   with small beakers might yield an accurate picture
   of the spray distribution.

3. It is recommended that a more detailed investigation
   be made of SAE 90 gear oil. The complete range of
   Spraying Systems orifice inserts for nozzle body
   Type SL should also be used. Specifically, higher
   temperature runs for this oil should be made so that
   lower values of viscosity can be obtained.

4. To ascertain the validity of equation (17) as a
   general correlation for most fluids used in the
   atomization process, considerable research is needed
   using a wide variety of fluids with viscosities
   ranging from approximately 1 to 500 centipoises.
   It is therefore recommended that SAE 90 gear oil be
   diluted to obtain viscosities near 10 centipoises
   for higher temperature runs. Also a full investigation
   of water is needed at low injection pressures, since
   data is available at pressures of 1000 psi and greater
   for nozzles of the same design.

5. The drag coefficient $\Delta P g_c / \rho \, v_o{}^2$ versus Reynolds number plot mentioned in the discussion of results should be investigated more fully in any future work as a means of correlating atomization data.

VIII Nomenclature

A = cross sectional area, ft.^{2}

C_p = specific heat, BTU/lb.-$^{\circ}$F

d = diameter, ft.

e = 2.718

f = a function

F_n = flow number, $Q/\sqrt{P}$

g_c = acceleration due to gravity, 32.17 ft./sec^2.

H = enthalpy, BTU's.

L = length, ft.

$P, \triangle P$ = injection pressure, lbs./ft^2.

q = time rate of growth of the amplitude of disturbance

Q = mass flow rate, lbs./sec.

Q' = heat added to system, ft.-lbs.

r = radius of curvature of differential element of fluid

R_o = initial jet radius

t = time, units as specified

T = temperature, $^{\circ}$F

v = velocity, ft./sec.

W' = shaft work, ft.-lbs.

Z' = work term due to elevation, ft.-lbs.

α_o = initial amplitude of disturbance

α = amplitude of disturbance at time t

σ = liquid surface tension

ρ = liquid density, lbs./ft^3.

μ = liquid viscosity, lbs.-mass/ft.-sec.

<u>constants</u>:

k, k', k'''

x, x', x''

z, z'

<u>exponents</u>:

$a, b, c, d, e, e', f, f', g, h, i, j, m, n, s$

<u>subscripts</u>:

c	=	air core
L	=	liquid
o	=	orifice
t	=	tangential
1	=	pre-nozzle liquid conditions
2	=	liquid conditions out of the orifice

IX BIBLIOGRAPHY

(1) Consiglio, J.A., and Sliepcevich, C.M., AICHE Journal, Vol. 3, No. 3, September 1957.

(2) Dumas, M., and Laster, R., Chem. Eng. Prog., Vol. 49, 518, (1953).

(3) Giffen, E., and Muraszew, A., The Atomization of Liquid Fuels, John Wiley & Sons, Inc., New York, (1953).

(4) Haelein, A., On The Disruption of a Liquid Jet, Forsch. Geb. Ingenieurwesens A, Vol. 2 No. 4, April 1931.

(5) Marshall, W.R., Jr., Atomization & Spray Drying, Chem. Eng. Prog. Monograph Series, Vol. 50, No. 2, (1954).

(6) McIrvine, J.D., M.S. Thesis, Univ. Wisconsin, (1953).

(7) Ohnesorge, W., Z. angew. Math. u. Mech., Vol. 16, 355, (1936).

(8) Ranz, W.E., On Sprays & Spraying, Bulletin No. 65, Dept. Eng. Research, Penn. State Univ., (1956).

(9) Rayleigh, Lord, Proc. London Math. Soc., Vol. 10, (1878).

(10) Tate, R.W., and Marshall, W.R., Jr., Chem. Eng. Prog., Vol. 49, 226, (1953).

X APPENDIX

A. Physical property measurements of SAE 90 gear oil:

1. Density:

The density of the oil was determined by specific gravity measurements using a hygrometer, calibrated at $60^{\circ}/60^{\circ}$. A water bath with a variable heat supply and a temperature control permitted constant temperature measurements to be taken over the desired temperature range, i.e. 90 to 194 $^{\circ}$F. The density of water with a specific gravity of 1.0000 is 62.368 lbs./ft^3. The specific gravity of the oil times 62.368, therefore, equals the density of the oil in lbs./ft^3. Refer to Figure (14) for a plot of the oil density versus temperature.

TABLE - 1

Temperature $^{\circ}$F	Specific gravity	Density lbs./ft^3
90	0.8762	54.647
105	0.8725	54.416
112	0.8696	54.235
120	0.8670	54.073
131	0.8635	53.855
140	0.8607	53.680
153	0.8567	53.431
165	0.8532	53.212
175	0.8500	53.013
189	0.8455	52.732
194	0.8441	52.645

FIGURE 14

DENSITY, LBS./FT³
VS.
TEMPERATURE, °F
FOR S.A.E. 90 OIL
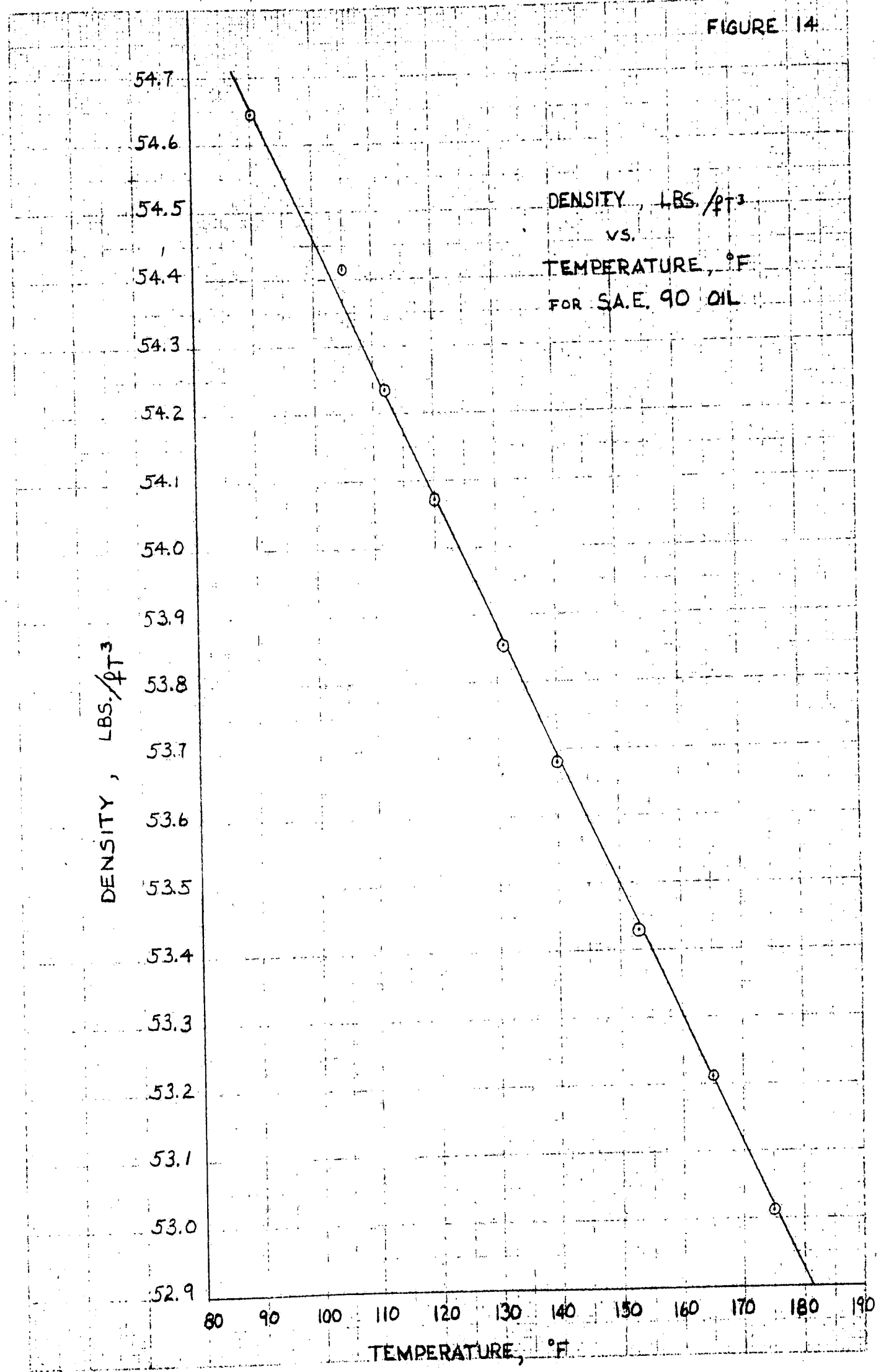
2. Viscosity:

A modified Ostwald Viscosity Pipette, number 200, was used to measure the oil viscosity. The procedure was to measure the time required for a definite volume of distilled water at constant known temperatures to fall through a capillary. The water bath mentioned in the density measurements was used to insure constant temperatures. Since the viscosity of pure water is known for the temperature range required in this investigation, the viscosity of the oil was determined, first, by measuring the time of efflux for the same volume of oil at the same temperatures as the water. Then, the viscosity of the water multiplied by the time ratio and a constant particular to the pipette yielded the value of the oil viscosity at the temperature of the run. Mathematically, the following procedure was used:

where:
CP = centipoises
CS = centistokes
SG = specific gravity

(a) $CS = CP/SG$

(b) $CS/time = C' =$ constant, particular to the pipette at the temperature of the run.

The constant C' was determined using distilled water at each temperature. The oil viscosity in centipoises was determined by solving (b) for CS and then (a) using C' and the time of effux for the oil at the particular temperature. Refer to Figure (15) for a plot of viscosity versus temperature for the oil.

FIGURE 15

VISCOSITY, CENTIPOISES
V.S.
TEMPERATURE, °F
OF SAE 90 GEAR OIL
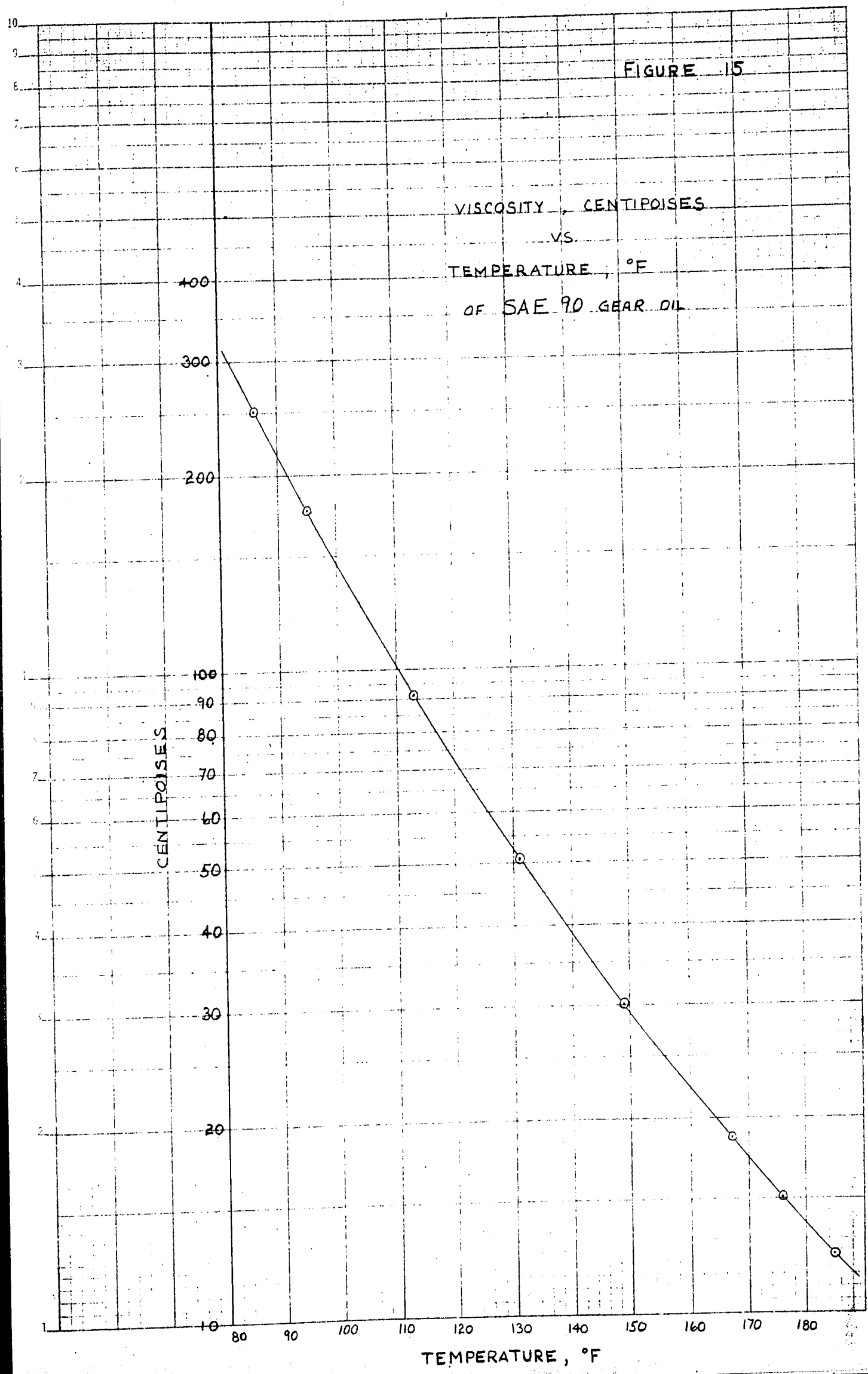
Table - 2 Viscosity determination

Water data:

Temp. °F	Time sec.	Specific gravity	Centipoises	Centistokes	Constant C'
86	12.0	0.9957	0.8007	0.8042	0.06701
95	11.2	0.9941	0.7225	0.7268	0.06489
113	10.1	0.9902	0.5988	0.6047	0.05987
131	9.2	0.9857	0.5064	0.5137	0.05584
149	8.6	0.9806	0.4355	0.4441	0.05164
167	8.2	0.9748	0.3799	0.3897	0.04752
185	7.8	0.9685	0.3355	0.3464	0.04441

SAE 90 gear oil:

Temp. °F	Time sec.	Specific gravity	Centistokes	Centipoises
86	4273	0.8775	286.4	251
95	3106	0.8747	201.6	176
113	1756	0.8691	105.2	91.4
131	1055	0.8635	58.9	50.9
149	680	0.8580	35.1	30.1
167	462	0.8525	21.9	18.7
185	328	0.8469	14.6	12.3
	281			

B. Underline:Equipment Specifications:

1. Agitator -

    Lightning Mixer, Mixing Equipment Co., Inc.,

    Rochester, N. Y.

        Model CV2, Serial No. 5713274, Type RR, Frame

        5217

        1/8 horse power, single phase, 115/230 volts,

        60 cycles, 3.4/1.7 amps.

2. Filter -

    Cuno Auto-Klean filter, Cuno Engineering Corporation,

    Meriden, Connecticut.

        pipe size = 1"

        continuously cleanable

        capacity, approximately 200 g.p.h.

        particles larger than 0.005" are filtered.

3. Motor -

    General Electric, 5 horse power

        Model 5K215BG229, No. 7M

        splash proof, air cooled, continuous

        3 phase, 220/440 volts, 14.2/7.1 amps

        60 cycles, 1745 R.P.M.

4. Nozzle and Related Equipment -

    Spraying Systems Co., Bellwood, Illinois

        swirl nozzle with removable orifice and core

        Body Type SL

orifice insert No.	core No.
50	10
54	16
58	17
65	20
72	21
80	27

orifice insert presses Nos. 1 and 3

5. Pressure gage -

   Ashcroft Test Gage

   0 to 3000 psi

6. Pump -

   Pesco Hydraulic Gear Pump, Pesco Products Division,

   Borg-Warner Corporation, Bedford, Ohio.

   Model 051001-060-01 - spline shaft

   rated capacity - 2.75 g.p.m. at 2000 p.s.i.

   and 1260 r.p.m.

   self lubricating

   weight 7.55 pounds

   recommended drive - chain and sprocket, Adapter

   041083 is needed to fit over the spline shaft.

7. Pump Adaptor 041083 -

   Automatic Transportation Company, Chicago 20 Illinois.

8. Sprocket and chain drive -

   No. 35 roller chain

   Boston Gears Nos. KSA19 and KSA24

9. Steam valve -

   American Precision Temp. Controller, Hajoca Corp.

   Bethlehem, Pa.

   Type 2242, size 1/2", bronze body, armored

tubing and copper bulb

temperature range 90 to 180°F

10. Thermocouple -

Conax Corporation, Buffalo, N. Y.

pressure gland, 3" immersion, copper-constantan

wire, 1/2" male threading

C. Data and Results:

1. Data:

Table - 3

Set I

Run	Pressure psig	Temperature millivolts	Time hrs.	Total flow rate lbs./hr.
32	300	2.25	0.1570	114.6
27	500	2.32	0.1667	132.0
28	700	2.33	0.1335	165.0
29	900	2.33	0.1225	179.5
31	1100	2.34	0.1102	199.5
33	1300	2.33	0.1289	217.0
36	1500	2.34	0.0883	227.0
38	1700	2.37	0.0835	239.5

Average temperature of set I = 134°F

Orifice insert used = No. 58

Core used = No. 20

Set II

Run	Pressure psig	Temperature millivolts	Time hrs.	Total flow rate lbs./hr.
52	900	1.25	0.0945	204.0
50	1100	1.35	0.0892	218.5
44	1300	1.37	0.0805	241.0
45	1500	1.39	0.0750	257.0
46	1700	1.39	0.0750	276.0
48	1900	1.41	0.0725	290.0

Average temperature of set II = 92°F

Orifice insert used = No. 58

Core used = No. 20

Table - 3 (cont'd)

Set III

Run	Pressure psig	Temperature millivolts	Time hrs.	Total flow rate lbs./hr.
53	500	1.22	0.0878	256.5
54	700	1.24	0.1000	316.0
56	900	1.32	0.1000	364.0
57	1100	1.29	0.0945	420.0
58	1300	1.25	0.0845	452.0
59	1500	1.33	0.0870	503.0
61	1800	1.39	0.0766	555.0

Average temperature of set III = 90°F

Ofifice insert used = No. 54

Core used = No. 21

Set IV

Run	Pressure psig	Temperature millivolts	Time hrs.	Total flow rate lbs./hr.
62	150	2.25	0.1333	146.0
63	250	2.25	0.1167	197.5
64	400	2.23	0.1167	249.0
67	600	2.28	0.1000	309.4
68	800	2.32	0.1000	349.4
69	1000	2.33	0.09170	396.0

Average temperature of set IV = 132.5°F

Ofifice insert used = No. 54

Core used = No. 21

Table - 4

Pounds/second collected

Run	Pressure psig	area 1	area 2	area 3	area 4
53	500	0.0657	0.00277	0.00099	0.00178
56	900	0.00818	0.00695	0.00226	0.0100
59	1500	0.0833	0.0244	0.0104	0.022
61	1800	0.0806	0.0335	0.0156	0.0242

Table 4 reports pounds of oil collected per second in each of the four equal areas situated under the nozzle. Figures (10), (11), (12), and (13) are plots of the pounds/sec. collected in each area versus distance from the nozzle axis. However the values are plotted as if they represented a point collection. For example, the weight rate collected in area 1 is plotted at 3.0", which is the periphery of area 1. The values from the other areas are treated in similar fashion.

2. Results:

Table - 5

Set I

Pressure psig	Flow rate lbs./sec.	Velocity ft./sec.
300	0.0318	61.5
500	0.0367	71.0
700	0.0458	88.5
900	0.0499	96.5
1100	0.0554	107.0
1300	0.0603	116.5
1500	0.0630	122.0
1700	0.0665	128.5

density = 53.795 lbs./ft^3

viscosity = 0.0313 $\frac{\text{lbs.-mass}}{\text{ft.-sec.}}$

orifice diameter = 0.0035 ft.

Set II

Pressure psig	Flow rate lbs./sec.	Velocity ft./sec.
900	0.0566	107.5
1100	0.0607	115.0
1300	0.0670	127.0
1500	0.0714	135.5
1700	0.0766	144.5
1900	0.0805	153.0

density = 54.609 lbs./ft^3

viscosity = 0.1345 $\frac{\text{lbs.-mass}}{\text{ft.-sec.}}$

orifice diameter = 0.0035 ft.

Set III

Pressure psig	Flow rate lbs./sec.	Velocity ft./sec.
500	0.0713	79.2
700	0.0878	97.5
900	0.1010	112.0
1100	0.1167	129.5
1300	0.1256	139.3
1500	0.1398	155.0
1800	0.1540	171.0

density = 54.647 lbs./ft^3

viscosity = 0.1446 $\frac{\text{lbs.-mass}}{\text{ft.-sec.}}$

orifice diameter = 0.00458 ft.

Set IV

Pressure psig	Flow rate lbs./sec.	Velocity ft./sec.
150	0.0405	47.1
250	0.0549	63.9
400	0.0692	80.5
600	0.0860	100.0
800	0.0970	112.8
1000	0.1100	128.0

density = 53.820 lbs./ft^3

viscosity = 0.0326 $\frac{\text{lbs.-mass}}{\text{ft.-sec.}}$

orifice diameter = 0.00458 ft.

Table 6

Set	Run	$\dfrac{d_o v_o \rho_L}{\mu_L}$	$\dfrac{\Delta P g_c}{\rho_L v_o^2}$	$\dfrac{Q}{\mu_L d_o}$	$\left(\dfrac{\Delta P g_c d_o^2 \rho_L}{\mu_L^2}\right) \times 10^5$
I	32	370	6.85	291	9.39
	27	427	8.60	335	15.7
	28	532	7.72	418	21.9
	29	580	8.33	456	28.1
	31	644	8.30	505	34.4
	33	700	8.25	552	40.7
	36	735	8.77	575	47.4
	38	744	8.89	609	53.3
II	52	152.5	6.60	120.7	1.54
	50	163.5	7.07	129.2	1.89
	44	180.2	6.82	142.5	2.23
	45	192.8	6.90	152.0	2.60
	46	207.0	6.85	163.0	2.92
	48	217.0	7.14	171.0	3.38
III	53	137.4	6.76	115.8	1.27
	54	169.0	6.25	142.5	1.78
	56	193.8	6.08	164.0	2.29
	57	224.0	5.55	189.3	2.80
	58	241.0	5.68	204.0	3.31
	59	268.0	5.35	227.0	3.85
	61	296.0	5.22	250.0	4.58
IV	62	356	5.88	288	7.45
	63	482	5.29	390	12.3
	64	607	5.32	490	19.6
	67	755	5.16	610	29.5
	68	850	5.43	689	39.3
	69	965	5.26	780	49.2

Table - 7

Temperature rise through the nozzle and viscosity correction:

Set I

Run	H_2 BTU/sec.	Temp. °F	Viscosity lbs.-mass ft.-sec.
32	0.0755	4.8	0.0269
27	0.100	5.4	0.0265
28	0.156	6.8	0.0255
29	0.186	7.4	0.0252
31	0.229	8.3	0.0245
33	0.267	8.8	0.0242
36	0.297	9.4	0.0238
38	0.329	9.9	0.0235

Set II

Run	H_2 BTU/sec.	Temp. °F	Viscosity lbs.-mass ft.-sec.
52	0.231	8.1	0.0981
50	0.264	8.7	0.096
44	0.322	9.6	0.0928
45	0.367	10.3	0.0900
46	0.423	11.0	0.0874
48	0.467	11.6	0.086

Set III

Run	H_2 BTU/sec.	Temp. °F	Viscosity lbs.-mass ft.-sec.
53	0.125	3.5	0.126
54	0.190	4.3	0.121
56	0.251	5.0	0.118
57	0.334	5.7	0.116
58	0.392	6.2	0.113
59	0.480	6.9	0.111
61	0.580	7.5	0.108

Set IV

Run	H_2 BTU/sec.	Temp. °F	Viscosity lbs.-mass ft.-sec.
62	0.0443	2.2	0.0306
63	0.0815	3.0	0.0299
64	0.129	3.7	0.0294
67	0.200	4.6	0.0286
68	0.254	5.2	0.0281
69	0.327	6.0	0.0275

Table - 8

Set	Run	$\dfrac{d_o v_o \rho_l}{\mu_l}$	$\left(\dfrac{\Delta P g_c d_o^2 \rho_l}{\mu_l^2}\right) \times 10^5$	$\dfrac{Q}{\mu_l d_o}$	$\left(\dfrac{Q}{\mu_l d_o}\right)\left(\dfrac{L}{d}\right)^{2/3} \times 10^3$
I	32	432	12.7	338	14.7
	27	505	21.9	394	17.1
	28	655	32.9	513	22.3
	29	722	43.4	565	24.6
	31	825	56.0	645	28.0
	33	910	67.9	712	31.0
	36	967	81.6	756	32.9
	38	1030	94.2	810	35.2
II	52	209	2.90	165	7.17
	50	229	3.70	181	7.87
	44	261	4.69	206	8.95
	45	288	5.80	226	9.83
	46	318	6.84	250	10.90
	48	340	8.28	267	11.60
III	53	157	1.69	123	4.47
	54	202	2.54	158	5.74
	56	237	3.44	187	6.80
	57	279	4.33	220	7.98
	58	309	5.40	243	8.82
	59	349	6.55	275	10.00
	61	394	8.24	311	11.30
IV	62	379	8.5	288	10.5
	63	526	14.7	401	14.5
	64	674	24.2	515	18.7
	67	860	39.4	658	23.9
	68	1070	53.0	753	27.3
	69	1150	69.4	875	31.8

D. <u>Sample Calculations:</u>

Calculations for run 32

1. Velocity through the nozzle, v_o.

$$v_o = Q/\rho A \quad \text{ft./sec.} \qquad \text{where: } \begin{array}{l} \rho = 53.795 \text{ lbs./ft.}^3 \\ A = 0.00000962 \text{ ft.}^2 \end{array}$$

$$v_o = \frac{0.0318}{(53.795)(0.00000962)} = 61.5 \text{ ft./sec.}$$

2. Temperature rise through the nozzle.

$$H_2 = \frac{v_2^2 - v_1^2}{2g_c} = \frac{\text{ft.-lbs.}}{\text{sec.}} \qquad \text{note: in all cases } v_1^2 \text{ is less than } 3.0 \text{ ft.}^2/\text{sec.}^2, \text{ therefore it will be neglected.}$$

hence,

$$H_2 = \frac{v_2^2}{2g_c} = \frac{(61.5)^2}{64.4} = \frac{3770}{64.4} = 58.5 \frac{\text{ft-lbs.}}{\text{sec.}}$$

$$\frac{58.5 \text{ ft.-lbs.}}{\text{sec.}} \times \frac{\text{BTU}}{778 \text{ ft.-lbs.}} = 0.0755 \text{ BTU/sec.}$$

finally,

$$\triangle T = \frac{H_2}{C_p Q} = \text{ }^{o}F \qquad \text{where: } C_p = 0.5 \frac{\text{BTU}}{\text{lb.-}^{o}F}$$

$$\triangle T = \frac{0.0755}{(0.5)(0.0318)} = 4.8 \text{ }^{o}F$$